

THE UNIVERSITY OF CHICAGO

DISCOVERY OF A NOVEL ROLE FOR SOG2 IN BUDDING YEAST MEIOSIS
USING A CONDITIONAL MUTANT SUPPRESSOR SCREEN

A THESIS SUBMITTED TO
THE FACULTY OF THE BIOLOGICAL SCIENCES DIVISION
AND THE BIOLOGICAL SCIENCES COLLEGIATE DIVISION
FOR THE COLLEGE UNDERGRADUATE HONORS PROGRAM

BY

LUCAS Y. TIAN

CHICAGO, ILLINOIS

MAY 2011

Tian

INTRODUCTION

Meiosis is a specialized form of cell division that produces four haploid gametes from a single diploid. Meiosis involves DNA replication followed by two rounds of chromosome segregation. The first round, in meiosis I (MI), segregates homologous chromosomes (reductional segregation), while the second round in meiosis II (MII) segregates sister chromatids in a similar fashion to mitosis (equational segregation). Interhomolog crossovers provide physical links between homologous chromosomes (homologs) that is necessary for high fidelity segregation. Thus, defects in interhomolog crossover can lead to inaccurate segregation and cell death. The former problem has clinical relevance since aneuploidies are the most common genetic cause of pregnancy loss and mental retardation in humans (Hassold & Hunt, 2001). Further, crossover events promote genetic diversity and are similar at the molecular level to the recombination based DNA repair process that is vital for mitotic genome stability. Defects in mitotic recombination can lead to breast cancer (van Gent et al., 2001).

We study meiosis in the budding yeast *Saccharomyces cerevisiae* for several reasons. First, meiotic recombination has been extensively studied in this organism. Second, many proteins involved in meiotic recombination are conserved from yeast across eukaryotes to humans. Third, the budding yeast's life cycle makes it amenable to studies of meiosis. *S. cerevisiae* can grow mitotically in both its haploid and diploid stages. A diploid is induced to sporulate, or undergo meiosis, when deprived of nutrients. Sporulation leads to formation of four ascospores in a tetrad contained in an ascus sac. The spores germinate when in optimal nutritional conditions and grow as haploid cells. When two haploids of opposite mating types are in close proximity they mate by fusing

Tian
to form a diploid (Herskowitz, 1988; Fig. 1). A major advantage of budding yeast is that spores from individual tetrads can be isolated using a micromanipulator. Then the segregation of genes from individual meiotic events can be analyzed. This technique is used frequently to construct recombinant haploids and in linkage analysis.

Crossover recombination is thought to follow the double strand break repair model (Szostak et al., 1983) (Fig. 2). Meiotic recombination is initiated by formation of double strand breaks (DSBs) catalyzed by the transesterase Spo11 (Keeney et al., 1997). At the site of the DSB both 5' DNA ends are resected by exonucleases to reveal 3' single stranded DNA (ssDNA). The following events require complex interactions between many different proteins. Strand exchange occurs, where the 3' strand invades the homologous duplex DNA to find a sequence of homology and forms Watson-Crick base pairs with the ssDNA. The homologous sequence acts as a template for DNA synthesis from the 3' ssDNA. DNA synthesis leads to formation of double Holliday junctions, which are generally resolved to form crossovers, but might sometimes lead to non-crossovers (Bishop & Zickler, 2004).

Crossover recombination requires the activity of Dmc1. *DMC1* is conserved across eukaryotes, and is a meiosis-specific homolog of the *Escherichia coli* recombination protein RecA. Strains lacking Dmc1 arrest late in meiotic prophase, accumulate double-strand break recombination intermediates, and cannot form proper synaptonemal complexes (SC), which are structures normally found between homologous chromosomes during MI (Bishop et al., 1992). Formation of the synaptonemal complex is closely tied with meiotic recombination, and one of the functions of the SC is to create constraints on recombination that promote *DMC1* mediated recombination (Bishop et al.,

Tian
1999; Schwacha & Kleckner, 1997). Dmc1p assembles into helical filaments on ssDNA at sites of recombinatory DSBs (Sehorn et al., 2004) and interacts with numerous accessory factor proteins to catalyze strand exchange.

Only a few Dmc1 accessory factor proteins have been characterized. Mei5-Sae3 is known to mediate the loading of Dmc1 onto ssDNA (Tsubouchi & Roeder, 2004). Hop2-Mnd1 is known to enhance DNA strand exchange, although it is unclear whether the effect is through a direct interaction with Dmc1p-ssDNA. Hop2-Mnd1 might help the invading 3' ssDNA find and bind to its ssDNA partner after the loading of the Dmc1 helical filament (Henry et al., 2006). Rad54 and Tid1 are members of the Swi/Snf family of translocases and, among other functions related to chromatin remodeling, are thought to promote the binding of Dmc1 to ssDNA over dsDNA. Dmc1 has high affinity for both ssDNA and dsDNA; Rad54 and Tid1 might catalyze the removal of Dmc1 from dsDNA (Petukhova et al., 1999; 2000; Holzen et al., 2006).

Since Dmc1p depends on accessory factors, we sought to study the molecular mechanism of recombination by finding more proteins that interact with Dmc1p. A conditional allele of *DMC1* was generated and a suppressor of that allele was found. It is hypothesized that the wild-type protein of the suppressor interacts either directly or indirectly with Dmc1 to regulate its activity.

Holzen (2005) mutagenized plasmids containing *DMC1* to create random *dmc1* alleles. She transformed the plasmids into a *dmc1Δ* mutant and selected for transformants that could sporulate at low, but not high temperatures. A *dmc1* allele that conferred that phenotype was named *dmc1-ts10*. *dmc1-ts10* mutants sporulate at around 75% wild-type efficiency at 24°C, but, just like *dmc1Δ* mutants, do not sporulate at 34°C.

Tian

Dmc1p is still expressed, but at 50% of wild type levels at 24°C and 30% at 34°C, and Dmc1 foci still form on DNA. However, it is not clear whether the Dmc1-ts10 protein has trouble associating specifically at sites of recombination.

Holzen then found suppressors by treating a *dmc1-ts10* mutant with a mutagen and selecting for suppression of the temperature-sensitive phenotype. Five complementation groups of suppressors were isolated. In this thesis we worked exclusively with the recessive suppressor *sup12*. *dmc1-ts10 sup12* diploids sporulated at about 10% efficiency of *DMC1* diploids at the restrictive temperature, and at 90% at the permissive temperature, which was higher than the *dmc1-ts10* single mutant (35%). *sup12* single mutants did not show a meiotic phenotype, and *sup12* haploids showed no phenotype as well.

Finding suppressors of conditional alleles has been a successful method for uncovering proteins that interact with the conditional allele *in vivo*. For example, the cell division cycle genes *CDC46/MCM5* and *CDC47/MCM7* were first found as suppressors of cold sensitive alleles of *CDC45* (Moir et al., 1982), and the actin-interacting genes *SAC1*, *VPS52/SAC2*, and *SAC3* were found as suppressors of a temperature-sensitive allele of the main actin gene *ACT1* (Novick et al., 1989). The logic behind the screen is that a defect in a pathway caused by a conditional mutation might be rescued by a compensatory suppressor mutation in another protein involved in the pathway. Genes identified in suppressor screens do not necessarily interact directly with the conditional allele and are less prone to false positives than screens for physically interacting proteins (Holzen, 2005). Suppressor screens are useful not only because they often reveal new players in biological pathways, but also because they allow identification of alleles that

Tian might not have a discernable phenotype as single mutants or might be lethal without a compensatory conditional mutation in another gene. Thus we hoped to find new proteins in the pathway of *DMC1* mediated recombination.

Because the suppressor does not bypass *dmc1Δ*, it is likely that the suppressor is involved in the Dmc1-dependent recombination pathway. Since *sup12* is recessive, it likely represents a loss of function, and so Holzen (2005) proposed that the wild-type suppressor protein might normally act to negatively regulate Dmc1. She proposed that the suppressor protein might normally negatively regulate assembly of Dmc1p onto chromatin, or might be a component of meiotic chromatin that places constraints on recombination. The latter case might lead to chromatin being more open and available for strand exchange in the suppressed state. Alternatively the suppressor protein might not be involved in recombination, but might help to stabilize the conditional Dmc1 mutant protein, for instance, as a folding chaperone (Zwick, 2008).

To find out what gene the suppressor mutation was in, Zwick (2008) first mapped *sup12* to chromosome XV using a set of chromosomal mapping strains. The mapping strains contained wild-type *SUP12*. When mated to a *sup12* strain the diploid would lose a specific chromosome that originated from the mapping strain (Wakem & Sherman, 1990). Because *sup12* is recessive, only when the chromosome containing the wild-type *SUP12* allele was lost would the *sup12* suppression phenotype be expressed, as the diploids always expressed the temperature-sensitive Dmc1 protein. Thus, by mating the suppressor strain to mapping strains corresponding to fifteen of the sixteen chromosomes, *sup12* was mapped to chromosome XV.

Tian

My thesis carries the work on from that point. We used linkage analysis between *sup12* and eight different chromosome XV markers to map *sup12* to a 20kb region. We sequenced the 20kb region to find two mutations that were unique to the *sup12* strain. One was in a non-coding region and the other truncated the C-terminus of *SOG2* by 65 amino acids. *SOG2* is an integral component of the RAM signaling network that is known to be involved in key mitotic processes such as maintenance of cell morphology and cytokinesis (Nelson et al., 2003), but has no known meiotic function. We showed that a *sog2* null mutation does not complement *sup12*, supporting the idea that *sup12* is an allele of *SOG2*. Further, *sog2Δ* strains have greatly reduced spore viability, indicating that they possess a meiotic defect. Combined with the fact that *sup12* mutants suppress the conditional *dmc1-ts10* mutant, we propose that *SOG2* might normally be involved in *DMC1* mediated recombination, possibly as a negative regulator. Also, the meiotic defects in *sog2Δ* mutants might reflect Sog2's possible role in meiotic recombination, or they might be caused by defects that are independent of Dmc1. For instance, deficiencies in actin localization might be responsible for the low spore viability of *sog2Δ* mutants.

Tian
METHODS

Yeast strains

All yeast strains used, apart from those in the Open Biosystems knockout (KO) collection, were isogenic SK1 derivatives (Table 1). The S288C MATa KO collection is available from Open Biosystems Products.

Strain Construction

Construction of linkage analysis strains by transformation

All linkage analysis marker strains (Table 1), except the *mek1* strain (DKB3528), were derived from strains in the Open Biosystems KO collection. DKB3528 was isolated as a recombinant spore from a cross between DKB3326 and DKB1931 followed by meiosis. *mek1Δ::NAT* was scored by growing spores on YPDA containing Nourseothricin, a fungicide that *NAT* confers resistance to. *dmc1-ts10* was scored by mating candidate spores that were known to be *dmc1Δ::ARG4* (from scoring on –Arg plates) with two *dmc1Δ* tester strains of opposite mating types, DKB793 and DKB794. The diploids formed from the *dmc1Δ* spores crossed with a tester strain were homozygous for *dmc1Δ*. If the spore was *dmc1-ts10*, then we expected to see sporulation at the permissive, but not the restrictive temperature. If the spore did not contain *dmc1-ts10*, then we expected no sporulation at any temperature. Sporulation was scored under light microscopy. Other mating and marker analysis techniques used are general to all experiments and are described below. From the DKB3326 x DKB1931 cross we derived two *mek1Δ* strains, DKB3528 and DKB3529.

Tian

The other marker strains were constructed in the following manner. Each strain in the KO collection has a known gene knocked out with *KANMX6*, which provides resistance to the fungicide Geneticin. The *markerΔ::KANMX6* cassette for each strain was amplified using PCR with the primers described in Table 2-1 (oliDB409–422; e.g. *pex11Δ::KANMX6* was amplified using oliDB409 and oliDB410). Primers were designed using the Primer BLAST website (<http://www.ncbi.nlm.nih.gov/tools/primer-blast/>) and Amplify 3X software and ordered from Integrated DNA Technologies. The primers were positioned such that, for each marker, at least one of the homology arms between the cassette and genomic DNA was at least 150bp long, and the other arm was at least 59bp long. Having at least one long homology arm allows for efficient transformation. The S288C genomic data was taken from the SGD Project (<http://www.yeastgenome.org/>) and SK1 genomic data was taken from the SGR Project (<http://www.sanger.ac.uk/research/projects/genomeinformatics/sgrp.html>). Genomic DNA preparation and PCR were performed as described below. The amplified products were transformed, using the protocol below, into DKB1931. We selected transformation that grew on YPDA (1% yeast extract, 2% Bacto-Peptone, 1% glucose, 0.001% Adenine solution, and 1% agar) plates containing Geneticin, and checked proper transformation using a PCR method. Genomic DNA was amplified using a forward primer (oliDB423–429) that bound upstream of the original two primers. The second primer used was the original reverse primer. Only if the construct transformed at the correct location on the genome would that combination of primers give the expected product. One correct strain from each transformation was saved and used for linkage analysis.

Tian

Construction of dmc1-ts10 sog2Δ double mutants by overlap PCR and transformation

SOG2 is not knocked out in the Open Biosystems KO collection because *sog2Δ* mutants are inviable in the S288C background (Nelson et al., 2003). Thus, we used overlap PCR to fuse a *KANMX4* cassette to homology arms that would allow it to target and replace the *SOG2* ORF during transformation. The *KANMX4* ORF was amplified from plasmid pNRB599 (pRS41K in Taxis & Knop, 2006; a gift from Nava Segev) using primers oliDB467 and oliDB468. The 0.5kb sequence ending immediately upstream of the *SOG2* ORF was amplified from DKB2604, the wild-type strain *sup12* was originally derived from, using oliDB469 and oliDB470. A second PCR reaction containing the two amplified products with no primers was used to fuse the two products. A third PCR reaction used the product from the second PCR step and the outer primers oliDB469 and oliDB468 to amplify the fusion cassette. The fused construct thus contained one 0.5kb homology arm that allowed efficient transformation. Because only one long homology arm is required for efficient transformation, we designed the other 40bp arm directly in the primer oliDB468. The PCR product was transformed into a *dmc1-ts10* diploid DKB2197. Correct targeting of transformation was checked using the PCR method described in the “Linkage analysis” section above, using oliDB471 and oliDB468. A correct transformant, DKB3589, was isolated and used in subsequent experiments. DKB3589 was sporulated to get haploid *sog2Δ* mutants (DKB3595 and DKB3596) of opposite mating types that were isogenic to each other and their parent (see tetrad plate in Fig. 8). We selected for markers by growing spores on plates missing single amino acids, as described below.

Tian

Construction of msc6Δ and mek1Δ strains used in the complementation test

A heterozygous *msc6Δ* mutant (DKB3592) was constructed by amplifying *msc6Δ::KANMX6* from the Open Biosystems KO Collection, using oliDB472 and oliDB473, and transforming the cassette into DKB2197. The methods used were analogous to those described for construction of the linkage analysis marker strains. OliDB474 was used as a new reverse primer to check proper transformation. DKB3592 was sporulated and two *dmc1-ts10 msc6Δ* haploids of opposite mating types (DKB3597 and DKB3598) were isolated.

The *mek1Δ* strains (DKB3528 and DKB3529) were first constructed for linkage analysis as described above.

Construction of sog2Δ single mutants

sog2Δ single mutants were constructed in both in the *ho* and the *HO* backgrounds. Both types were derived from the *dmc1-ts10 sog2Δ* strain constructed using transformation, described above. *HO* confers the homothallism phenotype, where a haploid will switch mating types and mate with its daughter after mitosis to form a diploid homozygous for all genes.

To construct the *ho sog2Δ* mutant, we mated the *dmc1-ts10 sog2Δ* haploid DKB3595 to both DKB3587 and DKB3588. We chose the latter two strains because they contain modified HIS4 loci that allow diploids to undergo a 2D gel analysis of joint-molecule recombination intermediates (Hunter & Kleckner, 2001). Diploids from both crosses were sporulated and *sog2Δ* single mutants were selected for. Three spores were chosen for use in future experiments: DKB3674, DKB3676, and DKB3679.

Tian

To construct the *HO sog2Δ* mutant, we mated DKB3676 with DKB17, which is homothallic and also contains a conditional mating allele *ste7-1*. *ste7-1* mutants mate with wild-type frequency at 24°C but are unable to mate at 34°C (McKee and Kleckner, 1997). That allele allowed us to grow *HO* haploids at high temperatures to create strains that could be saved as haploid and used for future crosses. The DKB3676 x DKB17 diploid was sporulated, tetrads were dissected and grown as usual, except they were grown for an extra day at 20°C to allow *HO ste7-1* spores to diploidize. We selected for *sog2Δ::KANMX4* spores by selecting for resistance to Geneticin. *sog2Δ* spores were then grown on YPDA for a day and transferred to SPM + 1/5 COM plates to assay for spore viability. The spore viability protocol is described below. *HO SOG2* spores were also isolated from this cross as controls for the spore viability experiment. Fig. 9 describes the logic behind the construction of the *HO* strains.

Growth, mating, and sporulation conditions

All strains were grown on YPDA plates (1% yeast extract, 2% Bacto-Peptone, 1% glucose, 0.001% Adenine solution, and 1% agar) at 30°C unless otherwise specified. Colonies were mated by mixing on YPDA and incubating at 30°C for 12 to 24 hours. Diploids were isolated by selection on double dropout plates as described below. We did not always isolate diploids when the next step was sporulation for strain construction or to assay spore viability. To induce sporulation, diploids were transferred to SPM + 1/5 COM plates (0.3% potassium acetate, 0.012% complete amino acid powder, 0.01% raffinose) and grown at 30°C for two to four days. Progression of sporulation was monitored by light microscopy.

Tian

Tetrad dissection

Tetrads were dissected after sporulating on SPM + 1/5 COM for at least two days.

Colonies of tetrads were transferred to a Zymolyase solution (0.27mg/ml Zymolyase 100T (US Biological) in ZK Buffer (25mM Tris pH7.5, 0.8M KCl)) and incubated for 15 minutes at 37°C to degrade the ascus sac around tetrads and kill vegetative cells.

Individual spores were separated using a micromanipulator microscope (Zeiss) and germinated on YPDA plates for three days at 30°C.

Testing for markers and mating type

Prototrophic and auxotrophic markers were scored by growing colonies on rich media plates missing one specific amino acid (dropout plates). Colonies were replicated to dropout plates after growing for at least a day on YPDA. We checked mating types of dissected tetrads by mating all spores to two tester strains of different mating types. The tester strain was chosen so that only diploids could survive on a specific double dropout plate. Double dropout plates lack two different amino acids, each one required by exactly one of the haploid mating strains, but neither required by the diploid. We selected for diploids by streaking the mating mixture on the double dropout plate.

Sporulation assay using dityrosine fluorescence

The presence of sporulation was detected in the linkage analysis and complementation tests by assaying for fluorescence of colonies. Spores, but not vegetative cells, contain a cell wall layer composed of dityrosine, which fluoresces under ultraviolet light (Briza et al., 1986). Colonies were first grown on YPDA for one day, then replica plated to a

Tian

YPDA plate with a nitrocellulose filter (S&S NC, 0.45 μ m pore size) placed between the agar and the cells. The filter facilitated the transfer of a large number of colonies from YPDA, after a day of growth, to SPM + 1/5 COM. Fluorescence was also more visible when the filter was present. 254nm and 365nm light were used interchangeably to induce spores to fluoresce blue light. A few colonies were also checked using light microscopy to confirm the accuracy of the fluorescence results. Fig. 7 shows an example of fluorescence.

Spore viability assay

Spore viability was assayed by dissecting tetrads with the method described above. Spores were germinated for at least three days on YPDA at 30°C, and spore viability was the proportion of spores that grew into visible colonies.

Linkage analysis

A *dmc1-ts10 sup12* mutant (DKB2702) was mated to each of the eight mapping strains (Table 1). Tetrads from the sporulated diploids were dissected and germinated. The pattern of co-segregation of *sup12* and the marker alleles indicated the recombination frequency between the two genes. Since *sup12* has no haploid phenotype, we scored *sup12* by first mating a plate of spores to two tester strains of opposite mating types. The tester strains (DKB3012 and DKB3013) were *dmc1-ts10 sup12* mutants. Therefore, only spores that were *sup12* would mate with a tester strain and form a diploid that showed the suppression phenotype. Mating was done by replica plating both the plate of tetrads and a plate saturated with a tester strain to a YPDA plate. After growing for one day the

Tian

mating plate was replica plated to a double dropout -Ura-Trp plate to select for diploids.

Diploid colonies were transferred to a YPDA plate and the dityrosine fluorescence assay

was performed as described above to determine *sup12* segregation. The segregation of

the mapping strain marker was assayed by replica plating spores to YPDA containing

Geneticin (or Nourseothricin for the *mek1* strain). The pattern of cosegregation within

each tetrad fell into one of three categories: parental ditype, non-parental ditype, and

tetratype (for an explanation see Fig. 3). The Perkins equation, frequency(cM) =

$50(T+6NPD)/(PD+NPD+T)$, (Perkins, 1949) was used to convert PD:NPD:T ratios into

recombination frequencies (calculated at <http://molbio.uoregon.edu/~fstahl/>).

Complementation test

All strains used in the complementation test were in a *dmc1-ts10* background. Diploids

were either constructed before for a different experiment or derived from crosses using

sog2Δ, *mek1Δ*, and *msc6Δ* strains whose construction methods have been described

above. The diploids that were constructed using mating methods were purified from their

haploid parents using one of two methods. When possible, double dropout plates were

used to select diploids (see above for method). Otherwise, diploids were selected by

isolating zygotes. Haploids were mated on YPDA. About six hours later a

micromanipulator was used to isolate dumbbell shaped cells that had presumably just

been formed from the fusion of two haploids. The cells were grown on YPDA for at least

two days. Zygotes were scored by the ability to sporulate at the permissive temperature,

using the dityrosine fluorescence assay. At least one zygote was isolated for each strain.

Tian

All diploids involved in the complementation test were then grown and sporulated together using the dityrosine fluorescence assay.

Molecular Biology

Genomic DNA preparation

Yeast genomic DNA was prepared using a spheroplast method previously described by Nasmyth & Reed (1980).

Transformation

Transformations were done using the LiAc/PEG method (Gietz & Woods, 2002). PCR products were first purified of primers and other PCR reagents using the Qiagen QIAquick PCR Purification Kit. About 2 μ g of DNA was used for each transformation. For each transformation, eight colonies that grew on YPDA with Geneticin, indicating presence of the gene construct, were streaked onto another YPDA (Gen) plate. After two days one colony was selected from each streak and grown on YPDA. DNA was prepared from each strain and diagnostic PCR was used to confirm correct transformation (see “Strain construction”).

PCR

PCR reactions that required high fidelity during strain construction and sequencing were performed using the Advantage 2 PCR Kit (Clontech) or the Pfu Turbo Polymerase (Stratagene). Diagnostic PCR was performed with the lower fidelity Titanium Taq PCR Kit (Clontech). We used the manufacturers’ recommended protocols. Kamino software was used to organize and design primers.

Tian

Sequencing

The 20kb region from base pair 996504 to 1016503 of chromosome XV from a *sup12* mutant DKB3518 and the wild-type strain it was derived from, DKB2604, was sequenced. SK1 genomic data was taken from the SGR Project. DKB3518 was produced after two rounds of backcrosses between *sup12* mutant DKB2677 and DKB2604. The backcrosses were done to reduce the background mutations from the mutagenesis procedure used construct DKB2677. Each round entailed mating a *sup12* haploid to DKB2604, sporulating and selecting a new *sup12* segregant. Five adjacent 4kb products, with at least 80bp overlap between adjacent products, were amplified using oliDB430 and oliDB434 for the first region, oliDB435 and oliDB439 for the second region, oliDB440 and oliDB444 for the third region, oliDB445 and oliDB449 for the fourth region, and oliDB450 and oliDB454 for the last region. Sequencing was performed at the University of Chicago Cancer Research Center (<http://cancer-seqbase.uchicago.edu>). Five different primers per region were initially used to sequence each region (oliDB430-434 for region 1, and so on). Some sections contained difficult sequences, such as polyT regions that might have caused instability in the DNA polymerase. To work around those regions oliDB455-460 were also used as sequencing primers. Sequencing results were analyzed using CLC Sequence Viewer 6.

RESULTS

***sup12* was mapped to a 20kb region of chromosome XV using linkage analysis**

Zwick (2008) had mapped *sup12* to chromosome XV (see Introduction). Subsequently, I used linkage analysis to map *sup12* to a specific region of chromosome XV. Eight mapping strains were constructed, each one replacing a gene along chromosome XV with another gene, *KANMX6*, that conferred resistance to the fungicide Geneticin. Each mapping strain was mated to a *dmc1-ts10 sup12* strain and meiotic progeny were analyzed to determine recombination frequency via tetrad analysis. The presence of *KANMX6* among ascosporal colonies was assayed by selecting for resistance to Geneticin. The presence of *sup12* could not be assayed directly from the haploid spores, since *sup12* has no known phenotype in haploids. Therefore, *sup12* was scored by mating all colonies to a *sup12 dmc1-ts10* test strain. Since *sup12* is recessive, only diploids homozygous for *sup12* would suppress the temperature sensitivity incurred by *dmc1-ts10*. Suppression of *dmc1-ts10* led to an ability to sporulate at both the permissive (20°C) and the restrictive (33°C) temperatures. We assayed for sporulation using the fact

Tian
that only spores contain a cell wall layer made of dityrosine, which fluoresces under ultraviolet light (Briza et al., 1986).

The Perkins equation (Perkins, 1949) was used to convert the ratio of frequency of three different marker segregation patterns (parental ditype, tetratype, and non-parental ditype) into a genetic map distance (see Fig. 3 for explanation).

The Open Biosystems knockout strain collection contained strains with the necessary markers knocked out with *KANMX6*. However, those strains could not be used as marker strains for two reasons. First they contained the wild-type allele of *DMC1*. It was necessary for both the *sup12* strain and the marker strains to have *DMC1* knocked out so that all segregants from mapping crosses would be *dmc1Δ*. The standard genotype of mapping diploids was *ade2/ADE2-dmc1-ts10, dmc1Δ/dmc1Δ, sup12/SUP12⁺, marker::KANMX6/MARKER⁺*. Haploid segregants from these diploids were crossed to haploid tester strains that were *dmc1-ts10 sup12*. Thus, only outcrossed diploids that were *sup12/sup12* would sporulate at the restrictive temperature. A second problem with the knockout strains was that they were in the S288C strain background, while the *sup12* strains were in the SK1 background. Differences in strain background can have profound effects on sporulation efficiency and S288C strains sporulate at very low efficiency compared to SK1.

To solve both problems with *KANMX6*-marked strains we used PCR to amplify the *KANMX6* with flanking sequences from the appropriate set of knockout strains, and then transformed the amplified gene construct into the genome of a *dmc1-ts10* strain in the SK1 background. We confirmed that transformation occurred at the marker's native position using PCR with one primer that annealed to a region inside the construct and a

Tian second primer that annealed outside the construct. We created eight mapping strains that spanned chromosome XV with intervals of approximately 160kb, or around 53cM using the average conversion factor of 3kb/cM along chromosome XV (SGD Project). That interval was used because it is less than the recombination frequency of 83cM that is calculated between two unlinked genes using the Perkins equation.

The results of linkage analysis indicated that *sup12* was about 43cM away from *MCH5*, 0cM away from *MEK1*, and 12cM away from *RAD17* (Table 3). We converted from genetic to physical distance using data from the SGD Project (www.yeastgenome.org). The database gives genetic and physical maps of each chromosome. Because there only exists genetic data for a few genes, we used *CPA1* and *RAD17* to calculate an average conversion factor for the region containing *MCH5*, *MEK1*, and *RAD17*. *CPA1* is 105kb to the left of *MCH5* and is the closest gene to *MCH5* that is annotated on the genetic map. Subtracting genetic distances, measured from the centromere, of *CPA1* and *RAD17* resulted in an approximate conversion factor between *CPA1* and *RAD17* of 2.72kb/cM, which is lower than the chromosome XV average of 3.0kb/cM. Using that factor we were able to map *sup12* to a 20kb region of approximate overlap between the 43cM sequence starting from *MCH5* and the 12cM sequence from *RAD17* (Fig. 4). That region of overlap contained the meiosis-specific kinase *MEK1*, as expected from the linkage value of 0cM between *mek1Δ* and *sup12*. Given that mutations in *MEK1* can bypass the arrest phenotype of a *dmc1Δ* mutant (Xu et al., 1997; Rockmill and Roeder, 1991), *MEK1* became a candidate for *SUP12* at this point in the analysis. The 20kb region also included *MSC6*, a gene that has a role in directing a

Tian
 meiotic cell to undergo interhomolog recombination more frequently than intersister
 recombination (Thompson & Stahl, 1999). Thus, *MSC6* was also a candidate for *SUP12*.

Sequencing revealed that *sup12* is an allele of *SOG2*

We sequenced the 20kb region centered at *MSC6* in a *sup12* mutant strain as well as the wild-type strain from which the mutant was derived. Because the *sup12* mutant was generated by EMS treatment, we completed two rounds of backcrosses between the *sup12* strain and the wild-type parent to reduce the number of background mutations. Each round entailed mating the *sup12* strain to the wild-type strain, inducing sporulation, and selecting a spore isogenic to the parent *sup12* strain.

The 20kb region was amplified into five adjacent 4kb sized PCR products, which were subsequently sequenced. We covered 94% of the sequence from both the *sup12* strain and its pre-mutagenesis parent. The only missed sequences that were in ORFs were the last 161bp of *MEK1* (plus 60bp directly downstream), and the first 298bp and base pairs 949-1068 of *YOR356W* (map at Fig. 5). Another 216bp that were not sequenced are in a non-coding region over 1kb upstream of *MSC6* and 651bp upstream of *GDO1*. Sequencing of some regions was hindered by polyT sequences, which presumably destabilized the DNA polymerase. We found two point mutations in the *sup12* mutant that were not present in the wild-type parent. One mutation was in *SOG2* and converted cytosine at base pair 2180 to thymine. When translated, the mutation converted tryptophan 727 to a stop codon, truncating the C-terminus by 65 amino acids. The second mutation was not in an ORF. Guanine was mutated to cytosine 92 base pairs

Tian upstream of the SNX3 ORF. *SOG2* has no known meiotic functions, but is known to be integral in the RAM signaling network (Nelson et al., 2003), described below.

The primary sequence of *SOG2* did not reveal any known protein domains in the last 65 amino acids of the protein, using both the Phyre2 program (Kelley & Sternberg, 2009; accessed at <http://www.sbg.bio.ic.ac.uk/phyre2/html/page.cgi?id=index>).

sog2Δ* did not complement *sup12

The logic behind the complementation test is explained in Fig. 6. In short, because *sup12* is recessive, *sup12/SUP12* did not suppress *dmc1-ts10* (i.e. *sup12* was complemented). However, if *sup12* is an allele of *SOG2*, then the suppression phenotype would be revealed in a *sup12/sog2Δ* diploid (i.e. lack of complementation). All strains were in a homozygous *dmc1-ts10* background. The suppression phenotype was considered present if sporulation could be detected at the restrictive temperature using the dityrosine fluorescence assay.

We could not construct a *SOG2* deletion strain by amplifying the *sog2Δ::KANMX6* cassette from the corresponding strain in the Open Biosystems knockout collection, since the *sog2Δ* strain is not present in the collection; *sog2Δ* mutants are inviable in the S288C strain background used for that collection (Nelson et al., 2003). Instead, we constructed the knockout by first using an overlap PCR method to create the gene construct, and then transforming it into yeast. Two rounds of PCR were used to fuse a *KANMX4* cassette to a PCR product containing a few hundred base pairs amplified from directly upstream of the *SOG2* ORF. The primer that was used at the other end of the *KANMX4* cassette contained a 40bp sequence homologous to the

Tian sequence directly downstream of *SOG2*. The two homology arms allowed transformation to replace the *SOG2* ORF with *KANMX4*. The resulting allele lacks *SOG2* function and allows the segregation of the *sog2Δ::KANMX4* mutant to be followed by resistance to Geneticin.

We performed the complementation analysis not only with *sog2Δ*, but also with knockouts of two other genes that are near *SOG2*. *MSC6* is directly upstream of *SOG2* and *MEK1* is the second gene downstream of *SOG2*. We constructed the *MSC6* knockout by amplifying *msc6Δ::KANMX6* from the knockout collection and then transforming into the desired SK1 strain. The *MEK1* knockout was derived by mating methods using a *mek1Δ::NAT* strain previously constructed in the lab. *NAT* confers resistance to fungicide Nourseothricin.

We found that *sog2Δ* did not, while *msc6Δ* and *mek1Δ* did complement *sup12* (Table 4 and Fig. 7). These results imply that *sup12* is an allele of *SOG2*, not of *MSC6* or *MEK1*, and support the results from sequencing. Importantly, all strains sporulated at the permissive temperature, indicating that the lack of sporulation of some strains at the restrictive temperature was caused by complementation of *sup12* by its wild-type allele, and not by a meiotic defect picked up during strain construction. We also observed suppression of *dmc1-ts10* in the *mek1Δ/mek1Δ* homozygous mutant diploid, which is not surprising considering that *mek1* mutants are known to bypass the need for Dmc1 during meiosis (Xu et al., 1997).

It is not conclusive whether *sog2Δ* suppressed *dmc1-ts10*

Tian

We obtained tentative results indicating that *sog2Δ* suppressed *dmc1-ts10*.

Because *sup12* is recessive, it was possible that truncation of the C-terminus of *SOG2* in that mutant resulted in a loss-of-function mutation, and thus conferred a phenotype which a complete knockout might display. The *sog2Δ/sog2Δ* strain used was identical to the one used in the complementation experiment above. Our results were not consistent between trials. In the first trial, sporulation of *dmc1-ts10 sog2Δ* diploids at 33°C was observed both by the dityrosine fluorescence assay, but very weakly, and under light microscopy. A second identical trial of the experiment did not show sporulation of *dmc1-ts10 sog2Δ* diploids at 33°C. This experiment will be repeated. Enough spores were present from the first trial to tentatively measure the diploid's spore viability at 33°C (see below).

***sog2Δ* mutants had varied morphological phenotypes**

SOG2 knockouts are inviable in some strain backgrounds, such as S288C. In the background used by our lab, SK1, *sog2Δ* strains were first created by transforming *sog2Δ::KANMX4* into a *dmc1-ts10* diploid background. All transformants presented with smaller colonies (Fig. 8) and cells than non-transformants. The mutant cells displayed the round morphology and clumping that has been described previously (Nelson et al., 2003).

sog2Δ strains in a wild-type *DMC1* background were created by crossing a *dmc1-ts10 sog2Δ* mutant to wild-type haploids and selecting for recombinant meiotic progeny with the desired genotypes. While all *sog2Δ* single mutants showed the expected round cell phenotype, they had a variety of colony sizes and cell sizes. The phenotype present

Tian did not seem to depend on other known mutations, since strains that were isogenic with respect to all known segregating markers regularly showed different size phenotypes. The phenotypes were likely the result of secondary suppressor mutations that increased competitive advantage from the slower growth and lower competitive fitness of *sog2Δ* mutants (Breslow et al., 2008). One piece of evidence is that *sog2Δ* mutants that were constructed as meiotic segregants of a *sog2Δ* heterozygote, which was formed by transformation, all had similarly small colonies (Fig. 8). That result it what we would expect, since a *sog2Δ* heterozygote would not display the decreased fitness that might promote accumulation of suppressors of *sog2Δ*. A second supporting result was that a cross between a *sog2Δ* mutant with normal sized colonies (DKB3676) and a wild-type strain (DKB17) gave both small and normal sized *sog2Δ* spores. Specifically, all 19 tetrads segregated 2:2 for *sog2Δ* and *SOG2*, with 16 tetrads displaying 1:1 segregation of small to large *sog2Δ* clones, and 3 tetrads having both *sog2Δ* ascosporal colonies showing the large phenotype. If there were an unlinked heterozygous secondary growth suppressor in the parent diploid we would expect a 1:1:4 ratio of tetrads showing the segregation patterns of *sog2Δ* spores being both large (parental-ditype):both small (non-parental ditype): one large, one small (tetraptype). The observed ratio did not differ significantly from the expected pattern from single unlinked suppressor (one-way Chi-squared test, p=0.132), but the sample size was too small to preclude the possibility of a more complex mode of suppression.. A third result showed that a purified small *sog2Δ* colony, when streaked onto YPDA, produced clones that grew into both large and small colonies (Fig. 10). The *sog2Δ* clone that was streaked been grown on YPDA for a few

Tian

days and stored at both 4°C and -80°C, after it had been isolated, which might have permitted accumulation of secondary suppressor mutations.

***dmc1-ts10 sog2Δ* diploids had low spore viability**

dmc1-ts10 sog2Δ diploids displayed greatly reduced spore viability compared to *dmc1-ts10 SOG2* diploids (Table 5). The viability of spores formed after meiosis was assayed by separating individual spores by micromanipulation and counting the proportion that successfully germinated. In the following text *sup12* is assumed to be an allele of *SOG2*, and the nomenclature of genotypes will reflect that assumption. All strains in this section are *dmc1-ts10* mutants. Meiosis at 20°C, the permissive temperature, led to wild-type levels of spore viability (>95%) for *sup12/SOG2* and *sog2Δ/SOG2* mutants. However, *sup12/sup12* diploids displayed slightly reduced spore viability at 88%; further, *sog2Δ/sog2Δ* mutants showed greatly reduced spore viability at 7%. *sog2Δ/sup12* diploids had 13% spore viability. At 33°C, spore viability could not be assayed for *SOG2/SOG2*, *sog2Δ/SOG2*, and *sup12/SUP12* diploids, because the *dmc1-ts10* background did not allow them to sporulate at that temperature. *sup12/sup12* mutants were able to sporulate and had 75% spore viability, *sog2Δ/sog2Δ* mutants had 15% spore viability, and *sog2Δ/sup12* diploids had 25% spore viability.

The tetrad viability patterns for *sup12 sog2Δ* double heterozygotes and *sog2Δ* homozygotes did not show 2:2 segregation of viability as we would expect if the defect was caused only by non-disjunction events at MI (see Table 5). The presence of 1-spore and 3-spore viable tetrads indicates that low viability might be caused by failure to

Tian

resolve lethal recombination intermediates, such as DNA double strand breaks, or defects at MII, such as spore formation or germination.

Larger *sog2Δ* single mutants had high spore viability, while smaller *sog2Δ* mutants have low spore viability

sog2Δ single mutants, all derived from mating and sporulating previously formed *sog2Δ* strains, formed colonies of various sizes. To measure spore viability, we first selected large and small *sog2Δ* clones that fit into two distinct groups based on cell and colony size. Large mutants were formed using two different genetic methods and small mutants using one method. Mating a wild-type haploid to the *dmc1-ts10 sog2Δ* haploids formed by transformation produced both large and small *sog2Δ* meiotic progeny. We isolated large *sog2Δ* colonies for use in future experiments, but small *sog2Δ* strains with the desired genotype were difficult to isolate because of difficulties with growing and mating in order to check their genotypes. Those difficulties led us to use a second method to construct small *sog2Δ* mutants.

Both large and small mutants were formed using a second method taking advantage of the homothallic property of the *HO* gene. Haploid strains expressing *HO* switch mating types after they undergo mitosis. The parent can then mate with the daughter, forming a diploid homozygous for all genes, including *sog2Δ* (Fig. 9). A second advantage of this method was that we did not need to separately construct haploid *sog2Δ* strains of opposite mating types. Further, mating two *sog2Δ* haploids was difficult because a phenotype of *sog2Δ* mutants is decreased efficiency in forming mating projections (Nelson et al., 2003). We presumed that homothallism reduced that problem

Tian by allowing haploids to be in close proximity before mating. Also, a reduction in the number of mating and growth steps was intended to minimize the chance for suppressor mutations that were suspected to convert small clones to large ones. We mated a large *ho sog2Δ* haploid to a *HO SOG2* haploid. We selected meiotic progeny from the resultant diploid that were *HO sog2Δ*, and allowed them to diploidize. We constructed both large and small *HO sog2Δ* strains using this method. Almost half of the *sog2Δ* segregants from this cross were small, even though the *sog2Δ* parent was large.

Large *sog2Δ* diploids in both *HO* and *ho* backgrounds had near wild-type levels of spore viability (Table 6). Large *HO sog2Δ* diploids displayed 93% spore viability, while large *ho sog2Δ* diploids had 95% spore viability. *sog2Δ/SOG2* diploids in an *ho* background had 94% spore viability. Small *sog2Δ* diploids were only constructed in the *HO* background; small *HO sog2Δ* diploids displayed 43% spore viability in one trial, and a repeat experiment found 11% spore viability (Table 6). The repeat experiment was done after freezing the strain at -80°C for storage and resuscitation by streaking on YPDA and selecting for small colonies. That ordeal, including differences in growth schedules that might have allowed more conversion of small *sog2Δ* mutants to large mutants in the first trial, might account for the difference in spore viability.

From the small *HO sog2Δ* diploid all of the 13 viable spores from the second trial were in tetrads with only one viable spore, a pattern that is inconsistent with a non-disjunction defect during MI. The latter would likely lead to a high proportion of two viable spore tetrads. The viability pattern of the small *ho sog2Δ* diploid also was not consistent with MI non-disjunction, and showed a wide distribution of 1,2,3, and 4-spore viable tetrads (Table 6).

DISCUSSION

***supI2* is an allele of *SOG2*, an integral component of the RAM signaling network**

We first mapped *supI2* to a 20kb region of chromosome XV using linkage analysis with eight different chromosome XV markers. The 20kb region was amplified and sequenced and a single nonsense mutation was found in *SOG2* in the *supI2* mutant, but not in the wild-type strain that *supI2* was derived from. The mutation truncated the C-terminus of

Tian
the 791 amino acid Sog2 protein by 65 residues. We confirmed the sequencing result by showing that a *sog2Δ* mutation did not complement *sup12*. Further, we showed that an *msc6Δ* and a *mek1Δ* haploid both complemented a *sup12* haploid, indicating that *sup12* is not an allele of *MSC6* or *MEK1*. The results for *MSC6* and *MEK1* are significant not only because those two genes are near *SOG2*, but also because they are known to be involved in meiotic recombination, and so were strong candidates for being *SUP12* prior to sequencing.

To provide further evidence that *SUP12* is *SOG2* we will use an overlap PCR method to construct a *sup12* cassette linking *KANMX4* to the *sog2* mutant allele that was found from sequencing. The construct would then be transformed into a *dmc1-ts10* mutant. We hope to show that transformants suppress the *dmc1-ts10* phenotype in a similar fashion to *sup12* mutants. We also plan to complete sequencing of the *MEK1* gene in the *sup12* mutant and determine if a plasmid expressing Sog2p can complement a *sup12* mutant, as we would expect if *SUP12* is *SOG2* and *sup12* is recessive. Also, as discussed in Results, we were not able to conclude that *sog2Δ* suppressed *dmc1-ts10*. Two experiments gave conflicting results. Showing that suppression indeed does occur would support the idea that *sup12* is a loss of function mutation, and that the last 65 amino acids of the C-terminus block recombination progression in *dmc1-ts10* diploids. On the other hand, if we show that *sog2Δ* does not suppress *dmc1-ts10*, then it would increase the chance that *sup12* is a gain-of-function mutation, possibly caused by the loss of a regulatory domain in the C-terminus (discussed below).

As discussed in the Introduction, the nature of the mutagenesis screens that identified *dmc1-ts10* and *sup12* make it highly probable that the wild-type protein

Tian expressed by *SUP12* is involved in *DMC1* mediated meiotic recombination. The fact that *sup12* suppresses *dmc1-ts10*, but not *dmc1Δ*, indicates that *sup12* probably acts through Dmc1-ts10 protein. Thus, the finding that *sup12* is an allele of *SOG2* implies that wild-type Sog2p might interact with *DMC1* or Dmc1p. Alternatively, the interaction could be indirect; Sog2p might be involved in negative regulation of Dmc1p, and thus explain why mutating Sog2p into Sup12p rescues Dmc1p function in a *dmc1-ts10* mutant at high temperatures. An important undertaking is to elucidate how Sog2p might interact with Dmc1p, and thus better understand the mechanism of Dmc1p mediated recombination.

Sog2p has no known meiotic functions. Sog2p is a leucine-rich repeat containing protein that is known to be an integral component of the RAM signaling network, which is involved in the timing of the transition from M1 to S phase (Bogomolnaya et al., 2006), maintaining actin localization during polarized growth (Weiss et al., 2002, Nelson et al., 2003), maintaining cell wall integrity (Kurischko et al., 2005), and initiating cytokinesis (Weiss et al., 2002). At least the latter three functions are mechanistically distinct. Five other proteins are known to be involved in the RAM network. Cbk1p, an NDR family kinase, acts downstream of all other RAM proteins (Nelson et al., 2003). Mob2p binds to Cbk1p and is necessary for its activity (Weiss et al., 2002). Tao3p is a scaffold protein that interacts with Mob2p-Cbk1p. Cbk1p activity depends on its phosphorylation by Kic1p (Nelson et al., 2003), a member of the PAK/Ste20 kinase family. Sog2p, Hym1p, and Kic1p bind to each other (Nelson et al., 2003). The activity of Cbk1p depends on all of the other RAM proteins (Jansen et al., 2006), but the molecular functions of Sog2p and Hym1p are unknown. Further, all RAM protein knockouts are inviable in the S288C strain background. In some backgrounds, such as

Tian
 W303 and SK1, they are viable, but have at least two distinct phenotypes: clumping of cells caused by dysfunctional cytokinesis, and an extremely round morphology. All members of the RAM network have orthologs in other eukaryotes, including humans (Bogomolnaya et al., 2006).

The diversity of functions that have been discovered for the RAM network and the relative dearth of literature on *SOG2* create optimism that our two main conclusions (an allele of *SOG2* suppresses a temperature-sensitive *DMC1* mutant, and *sog2Δ* mutants have low spore viability) indicate a novel meiotic function of Sog2p. For instance, Sog2p might be necessary for proper segregation of homologous chromosomes during MI, or of sister chromatids during MII. Those defects can cause aneuploidy, which would explain the low spore viability. That scenario makes even more sense when considering that the nature of the mutagenesis screen for *sup12* suggests that Sog2p interacts with *DMC1*. If that were the case, knocking out *SOG2* might cause a defect in crossover recombination and impair accurate segregation of homologs during MI.

It is also possible that *SOG2* is normally involved in a meiotic checkpoint that inhibits progress until conditions are right. Then, it would make sense that a mutation in *SOG2* might bypass the meiotic arrest of a *dmc1-ts10* mutant. If the presence of the checkpoint depends on the presence of Dmc1p filaments, then we would expect *sog2* mutants to suppress *dmc1-ts10*, which forms such filaments, but not suppress *dmc1Δ*, as was observed. It is known that the lack of Dmc1 stimulates a Mec1- and Mek1-dependent checkpoint that leads to prophase I arrest (Lydall et al., 1996; Xu et al., 1997). Thus, in a *dmc1-ts10* mutant formation of Dmc1 filaments might allow progression from that checkpoint to a later one that depends on the activity of the Sog2 C-terminus. A

Tian
sup12 mutant might thus bypass a Sog2-mediated arrest. However, that bypass would not be expected to produce a high proportion of viable spores, which we observed in homozygous *sup12* diploids. It is known that bypassing the *MEC1* and *MEK1* mediated checkpoint through mutations in those genes leads to low spore viability (Lydall et al., 1996; Rockmill & Roeder, 1991). A possible explanation for the high spore viability of *sup12* mutants is that a Sog2-mediated checkpoint responds to accumulation of Dmc1p filaments on non-recombinatory dsDNA, and bypassing that checkpoint allows MI to still complete with most of the DSBs repaired, because a high proportion of the Dmc1 filaments might be localized at DSBs. To test this hypothesis we need to first determine whether Dmc1-ts10 protein accumulates on non-recombinatory dsDNA. However, it is unclear how a role for Sog2 in such a recombination checkpoint might lead to the low spore viability we showed in Sog2 knockouts.

SOG2 may be involved in other meiotic processes, such as spore wall formation or trafficking of mitochondria (discussed below), or reduced cell integrity. An inability of spores to germinate or grow if they are *sog2Δ* seems unlikely considering the fact that spore viability of *sog2Δ/SOG2* diploids in both *DMC1* (Table 6) and *dmc1-ts10* (Table 5) backgrounds were similar to wild-type levels.

Two experiments currently underway, described under “Future directions,” would help pinpoint whether *SOG2* is indeed involved in MI. Construction of a meiosis-specific *SOG2* knockout would remove vegetative defects found in the full knockout, and a strain in a *spo11 spo13* background would make viable spores without the need for proper crossover during MI. Thus, a *spo11 spo13 sog2Δ* diploid would have wild-type levels of spore viability if the meiotic function of *SOG2* is only required for meiotic recombination

Tian and reductional segregation, not for premeiotic DNA synthesis, equational segregation or spore formation (Malone and Esposito, 1981).

The actin localization defect found in *sog2Δ* mutants might play a role in its meiotic defects. Actin has been implicated in chromosomal segregation (Palmer et al., 1992), sporulation, and nuclear segregation (Whitacre et al., 2001). Actin patches are essential for the subsequent maturation of the spore wall chitosan and dityrosine layers, and cells treated with the actin depolymerizing agent Latrunculin A do not form spores (Taxis et al., 2006). In *Schizosaccharomyces pombe* Mug27 is a member of the conserved NDR kinase family that includes the RAM network kinase Cbk1p. Supporting the hypothesis that the RAM network regulates spore PSM and spore wall formation, Mug27 regulates forespore membrane (PSM in *S. cerevisiae*) formation, although the mechanism is unknown. Just as in *sog2Δ* mutants, *mug27Δ* mutants had less than 50% spore viability (Ohtaka et al., 2008). In *S. cerevisiae*, the actin cytoskeleton also controls movement and inheritance of mitochondria during mitosis (Drubin et al., 1993) and meiosis (Smith et al., 1995). For the above reasons it is thus plausible that actin localization defects in *sog2Δ* mutants might lead to low spore viability.

Because *sup12* mutants do not display the mitotic phenotypes of *sog2Δ* mutants, the last 65 amino acids of the C-terminus of Sog2 are likely not required for its mitotic function, assuming that *SUP12* is *SOG2*. Thus, it is possible that the *DMC1*-related function of Sog2 and its mitotic functions are separate. One could imagine a scenario where the C-terminus of *SOG2* is a site of regulation of its *DMC1*-related function. Although *sup12* seems to be recessive, it is possible that it is also a gain-of-function allele, with the presence of normal protein acting to block the function gained by the

Tian mutant protein. Future experiments will address whether overexpression of *sup12* in the presence of *SUP12* can lead to the suppression phenotype. Also, to check whether the *sup12* suppression phenotype might be specifically caused by loss of the C-terminus, we are sequencing other suppression alleles from the *sup12* complementation group, *sup4* and *sup6*, that were found in the original mutagenesis screen by Holzen (2005). First, finding mutations in *SOG2* in both of those mutants would support the argument that *SUP12* is identically *SOG2*. Second, knowing the specific type of mutation might also reveal whether a specific allele, such as one with a truncated C-terminus, and not loss-of-function alleles in general, might be involved in suppression of *dmc1-ts10*, and provide further insight into the mechanism of suppression.

The growth defects of *sog2Δ* mutants likely led to secondary suppression mutations

Different *sog2Δ* single mutants had different sized colonies and cells. The clones with the largest colonies showed wild-type spore viability levels, while small clones had low spore viability. It is likely that the fitness defects of *sog2Δ* increased the occurrence of advantageous suppressor mutations. That idea was supported by evidence that a newly transformed *sog2Δ* heterozygote produced tetrads from which all *sog2Δ* ascospores displayed the small phenotype (Fig. 8). That result supports the argument that a heterozygote without noticeable fitness defects should not accumulate suppressor mutations. A second important result was that small *sog2Δ* segregants were found from a cross between a large *sog2Δ* mutant and a wild-type strain, which is to be expected if one or more extragenic suppressors were causing the different growth phenotypes, rather than mutations or epigenetic modification of the *SOG2* gene (schematic in Fig. 9).

Tian

Suppressors of RAM network mutations have been found before. Others have shown that the poor cell integrity and slow growth phenotypes of *kic1Δ* and *ckb1Δ*, RAM network knockouts, have improved over time when grown on rich media, probably due to accumulation of suppressor mutations (Kurischko et al., 2005; Vink et al., 2002). Further, at least one suppressor of *sog2Δ* has already been characterized. *ssd1* mutants are known to be suppressors of the inviability caused by all RAM network member knockouts in the S288C background (Nelson et al., 2003). *Ssd1* might normally function in controlling cell integrity (Kurischko et al., 2005).

It would be beneficial to avoid the variation in *sog2Δ* phenotypes for three reasons. First, results derived from strains with such high phenotypic variance might not reflect the normal function of Sog2p if the variance stems from suppressor mutations. Further if there is an epigenetic basis for the suppression, strains constructed using mating methods might accumulate epigenetic modifications that make it difficult to isolate the effects of Sog2 deficiency. Third, the small *sog2Δ* strains are difficult to culture because they grow slowly and are not efficient at mating. We are thus in the process of constructing a meiosis-specific *SOG2* knockout, as described below, which would allow normal non-meiotic growth.

Future directions

We are currently constructing a meiosis-specific *SOG2* knockout, which will have *SOG2* driven by the *CLB2* promoter. *CLB2* is involved in cell cycle progression and is expressed during mitosis, but is repressed during meiosis (Grandin et al., 1993). The system has been used successfully by others, including Lee and Amon (2003), who

Tian showed that the normally meiotically expressed proteins Cdc5p and Cdc20p were completely absent from cell extracts after less than two hours of meiosis, when driven by the *CLB2* promoter.

Using the *pCLB2-SOG2* mutant we plan to construct a *spo11 spo13 pCLB2-SOG2* diploid. *spo11 spo13* mutants synthesize sister chromatids, but bypass MI and the requirement for recombination and only undergo one equational division to form viable diploid spores (Malone and Esposito, 1981). If we do not find any difference in spore viability between *spo11 spo13 pCLB2-SOG2* diploids and *spo11 spo13 SOG2* controls, and if *pCLB2-SOG2* diploids exhibit low spore viability similar to *sog2Δ* mutants, then we can conclude that *SOG2* is involved in MI and possibly recombination.

We will also use a 2D gel electrophoresis system to characterize branched joint DNA recombination intermediates (Hunter & Kleckner, 2001) in a *pCLB2-SOG2* and in a *dmc1-ts10 sup12* mutant. That assay allows us to characterize the recombination intermediates and to determine the ratio of interhomolog to intersister recombination (IH:IS). Previous studies have shown that recombination in the absence of Dmc1 leads to a low IH:IS ratio (Schwacha & Kleckner, 1997). Measuring IH:IS for *dmc1-ts10 sup12* mutants will thus indicate whether suppression is restoring normal Dmc1 mediated recombination, or occurring by a pathway dependent on intersister recombination.

ACKNOWLEDGEMENTS

Doug Bishop was a constant guiding presence that provided influential mentorship and advice not only this project, but also on my career. Daniil Gataulin and Raphaelle Laureau assisted with the linkage analysis experiments. R.L. also performed the backcrosses before the sequencing of the *sup12* strain. Other members of the Bishop lab,

Tian
especially Ling Chen and Jennifer Grubb, assisted at numerous points during the project.

My thesis advisors, D.B., Ben Glick, and Stephen Kron, gave helpful comments on this thesis.

REFERENCES

- Bishop, D K, Nikolski, Y., Oshiro, J., Chon, J., Shinohara, M., & Chen, X. (1999). High copy number suppression of the meiotic arrest caused by a dmc1 mutation: REC114 imposes an early recombination block and RAD54 promotes a DMC1-independent DSB repair pathway. *Genes to cells*, 4(8), 425-44.
- Bishop, D K, Park, D., Xu, L., & Kleckner, N. (1992). DMC1: a meiosis-specific yeast homolog of E. coli recA required for recombination, synaptonemal complex formation, and cell cycle progression. *Cell*, 69(3), 439-456.

Tian

Bishop, Douglas K., & Zickler, D. (2004). Early decision; meiotic crossover interference prior to stable strand exchange and synapsis. *Cell*, 117(1), 9-15.

Bogomolnaya, L. M., Pathak, R., Guo, J., & Polymenis, M. (2006). Roles of the RAM signaling network in cell cycle progression in *Saccharomyces cerevisiae*. *Current genetics*, 49(6), 384-92.

Breslow, D. K., Cameron, D. M., Collins, S. R., Schuldiner, M., Stewart-Ornstein, J., Newman, H. W., et al. (2008). A comprehensive strategy enabling high-resolution functional analysis of the yeast genome. *Nature methods*, 5(8), 711-8.

Briza, P., Winkler, G., Kalchhauser, H., & Breitenbach, M. (1986). Dityrosine is a prominent component of the yeast ascospore wall. A proof of its structure. *The Journal of biological chemistry*, 261(9), 4288-94.

Drubin, D. G., Jones, H. D., & Wertman, K. F. (1993). Actin structure and function: roles in mitochondrial organization and morphogenesis in budding yeast and identification of the phalloidin-binding site. *Molecular biology of the cell*, 4(12), 1277-94.

Gent, D. C. van, Hoeijmakers, J. H., & Kanaar, R. (2001). Chromosomal stability and the DNA double-stranded break connection. *Nature reviews. Genetics*, 2(3), 196-206.

Gietz, R. D., & Woods, R. a. (2002). Transformation of yeast by lithium acetate/single-stranded carrier DNA/polyethylene glycol method. *Methods in enzymology*, 350(2001), 87-96.

Grandin, N., & Reed, S. I. (1993). Differential function and expression of *Saccharomyces cerevisiae* B-type cyclins in mitosis and meiosis. *Mol. Cell. Biol.*, 13(4), 2113-2125.

Hassold, T., & Hunt, P. (2001). To err (meiotically) is human: the genesis of human aneuploidy. *Nature reviews. Genetics*, 2(4), 280-91.

Henry, J. M., Camahort, R., Rice, D. A., Florens, L., Swanson, S. K., Washburn, M. P., et al. (2006). Mnd1/Hop2 facilitates Dmc1-dependent interhomolog crossover formation in meiosis of budding yeast. *Mol Cell Biol*, 26(8), 2913-2923.

Herskowitz, I. (1988). Life cycle of the budding yeast *Saccharomyces cerevisiae*. *Microbiological reviews*, 52(4), 536-53.

Holzen, T. M., Shah, P. P., Olivares, H. A., & Bishop, Douglas K. (2006). Tid1/Rdh54 promotes dissociation of Dmc1 from nonrecombinogenic sites on meiotic chromatin. *Genes Dev*, 20(18), 2593-2604.

Holzen, T. (2005). Identification of factors that regulate the meiosis-specific recombinase Dmc1. *PhD dissertation*, The University of Chicago

Tian

Hunter, N., & Kleckner, N. (2001). The single-end invasion: an asymmetric intermediate at the double-strand break to double-holliday junction transition of meiotic recombination. *Cell*, 106(1), 59-70.

Jansen, J. M., Barry, M. F., Yoo, C. K., & Weiss, Eric L. (2006). Phosphoregulation of Cbk1 is critical for RAM network control of transcription and morphogenesis. *The Journal of cell biology*, 175(5), 755-66.

Keeney, S., Giroux, C. N., & Kleckner, Nancy. (1997). Meiosis-Specific DNA Double-Strand Breaks Are Catalyzed by Spo11, a Member of a Widely Conserved Protein Family. *Cell*, 88(3), 375-384.

Kelley, L.A., & Sternberg, M.J.E. (2009). Protein structure prediction on the Web: a case study using the Phyre server. *Nature Protocols*, 4(3), 363-371.

Kurischko, C., Weiss, G., Ottey, M., & Luca, F. C. (2005). A role for the *Saccharomyces cerevisiae* regulation of Ace2 and polarized morphogenesis signaling network in cell integrity. *Genetics*, 171(2), 443-55.

Lee, B. H. (2003). Role of Polo-like Kinase CDC5 in Programming Meiosis I Chromosome Segregation. *Science*, 300(5618), 482-486.

Lydall, D. & Weinert, T. (1996). From DNA damage to cell cycle arrest and suicide: a budding yeast perspective. *Current Opinion in Genetics & Development*, 6(1), 4-11.

Malone, R. E., & Esposito, R. E. (1981). Recombinationless meiosis in *Saccharomyces cerevisiae*. *Molecular and cellular biology*, 1(10), 891-901.

McKee, A. H., & Kleckner, N. (1997). A general method for identifying recessive diploid-specific mutations in *Saccharomyces cerevisiae*, its application to the isolation of mutants blocked at intermediate stages of meiotic prophase and characterization of a new gene SAE2. *Genetics*, 146(3), 797-816.

Moir, D., Stewart, S. E., Osmond, B. C., & Botstein, D. (1982). Cold-sensitive cell-division-cycle mutants of yeast: isolation, properties, and pseudoreversion studies. *Genetics*, 100(4), 547-63.

Nasmyth, K. A. (1980). Isolation of Genes by Complementation in Yeast: Molecular Cloning of a Cell-Cycle Gene. *Proceedings of the National Academy of Sciences*, 77(4), 2119-2123.

Nelson, B., Kurischko, C., Horecka, J., Mody, M., Nair, P., Pratt, L., et al. (2003). RAM: a conserved signaling network that regulates Ace2p transcriptional activity and polarized morphogenesis. *Mol Biol Cell*, 14(9), 3782-3803.

Novick, P., Osmond, B. C., & Botstein, D. (1989). Suppressors of yeast actin mutations. *Genetics*, 121(4), 659-74.

Tian

Ohtaka, A., Okuzaki, D., & Nojima, H. (2008). Mug27 is a meiosis-specific protein kinase that functions in fission yeast meiosis II and sporulation. *Journal of cell science*, 121(9), 1547-58.

Petukhova, G., Van Komen, S., Vergano, S., Klein, H., Sung, P. (1999). Yeast Rad54 promotes Rad51-dependent homologous DNA pairing via ATP hydrolysis-driven change in DNA double helix confirmation. *J. Biol. Chem.* 262, 1337-43.

Petukhova, G., Sung, P., Klein, H. (2000). Promotion of Rad51-dependent D-loop formation by yeast recombination factor Rdh54/Tid1. *Genes and Dev.* 14, 2206-15.

Palmer, R., Sullivan, D., Huffaker, T., & Koshland, D. (1992). Role of Astral Microtubules and Actin in Spindle Orientation and Migration in the Budding Yeast. *The Journal of cell biology*, 119(3), 583.

Perkins, D. D. (1949). Biochemical mutants in the smut fungus Ustilago maydis. *Genetics*, 34(5), 607-26.

Read, L. R., Raynard, S. J., Rukść, A., & Baker, M. D. (2004). Gene repeat expansion and contraction by spontaneous intrachromosomal homologous recombination in mammalian cells. *Nucleic acids research*, 32(3), 1184-96.

Rockmill, B., & Roeder, G. S. (1991). A meiosis-specific protein kinase homolog required for chromosome synapsis and recombination. *Genes & development*, 5(12B), 2392-404.

Schwacha, A., & Kleckner, N.. (1997). Interhomolog Bias during Meiotic Recombination: Meiotic Functions Promote a Highly Differentiated Interhomolog-Only Pathway. *Cell*, 90(6), 1123-1135.

Sehorn, M. G., Sigurdsson, S., Bussen, W., Unger, V. M., & Sung, P. (2004). Human meiotic recombinase Dmc1 promotes ATP-dependent homologous DNA strand exchange. *Nature*, 429(6990), 433-7.

Smith, M. G., Simon, V. R., O'Sullivan, H., & Pon, L. a. (1995). Organelle-cytoskeletal interactions: actin mutations inhibit meiosis-dependent mitochondrial rearrangement in the budding yeast *Saccharomyces cerevisiae*. *Molecular biology of the cell*, 6(10), 1381-96.

Szostak, J. W., Orr-Weaver, T. L., Rothstein, R. J., & Stahl, F. W. (1983). The double-strand-break repair model for recombination. *Cell*, 33(1), 25-35.

Taxis, C., & Knop, M. (2006). System of centromeric, episomal, and integrative vectors based on drug resistance markers for *Saccharomyces cerevisiae*. *BioTechniques*, 40(1), 73-78.

Tian

- Taxis, C., Maeder, C., Reber, S., Rathfelder, N., Miura, K., Greger, K., et al. (2006). Dynamic organization of the actin cytoskeleton during meiosis and spore formation in budding yeast. *Traffic*, 7(12), 1628-42.
- Thompson, D. A., & Stahl, F. W. (1999). Genetic control of recombination partner preference in yeast meiosis. Isolation and characterization of mutants elevated for meiotic unequal sister-chromatid recombination. *Genetics*, 153(2), 621-641.
- Tsubouchi, H., & Roeder, G Shirleen. (2004). The budding yeast mei5 and sae3 proteins act together with dmc1 during meiotic recombination. *Genetics*, 168(3), 1219-30.
- Vink, E., Vossen, J. H., Ram, A. F. J., Ende, H. van den, Brekelmans, S., Nobel, H. de, et al. (2002). The protein kinase Kic1 affects 1,6-beta-glucan levels in the cell wall of *Saccharomyces cerevisiae*. *Microbiology*, 148, 4035-48.
- Wakem, L. P., & Sherman, F. (1990). Chromosomal assignment of mutations by specific chromosome loss in the yeast *Saccharomyces cerevisiae*. *Genetics*, 125(2), 333-40.
- Weiss, E. L. (2002). The *Saccharomyces cerevisiae* Mob2p-Cbk1p kinase complex promotes polarized growth and acts with the mitotic exit network to facilitate daughter cell-specific localization of Ace2p transcription factor. *The Journal of Cell Biology*, 158(5), 885-900.
- Whitacre, J., Davis, D., Toenjes, K., Brower, S., & Adams, a. (2001). Generation of an isogenic collection of yeast actin mutants and identification of three interrelated phenotypes. *Genetics*, 157(2), 533-43.
- Xu, L., Weiner, B. M., & Kleckner, N. (1997). Meiotic cells monitor the status of the interhomolog recombination complex. *Genes & Development*, 11(1), 106-118.
- Zwick, D. (2008). Mapping suppressors of a conditional dmc1 allele. *Undergraduate Honors Thesis*, The University of Chicago.

FIGURES

Tian

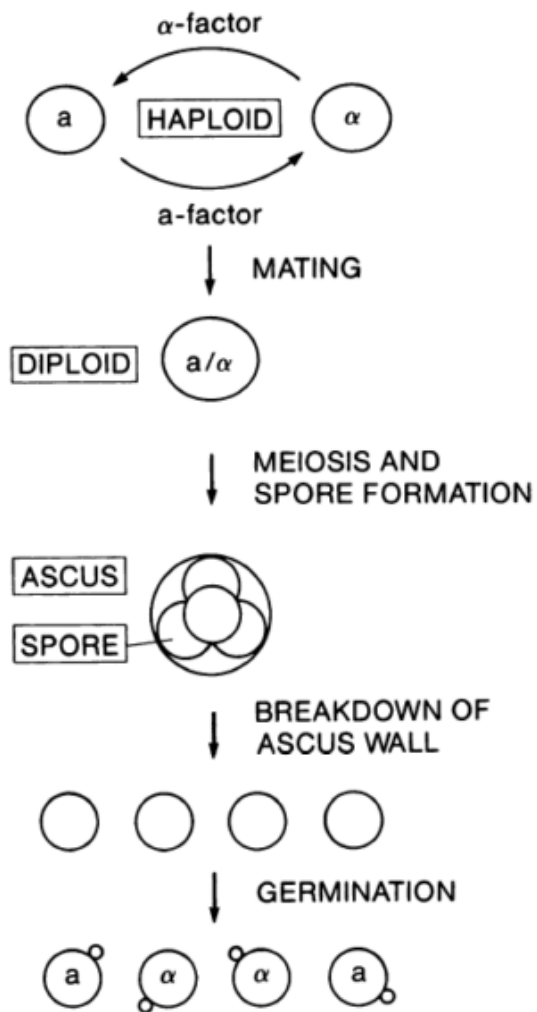


Figure 1. The life cycle of *S. cerevisiae*. Haploids exist as one of two mating types, **a** and **α**. Haploids will mate when in proximity to form **a/α** diploids. All three cell types can grow mitotically. Diploids can undergo meiosis to form a tetrad, which consists of four haploid spores surrounded by an ascus membrane. The ascus can be degraded enzymatically and the four spores can be micromanipulated, germinated, and analyzed individually. (Figure from Herskowitz, 1988)

Tian

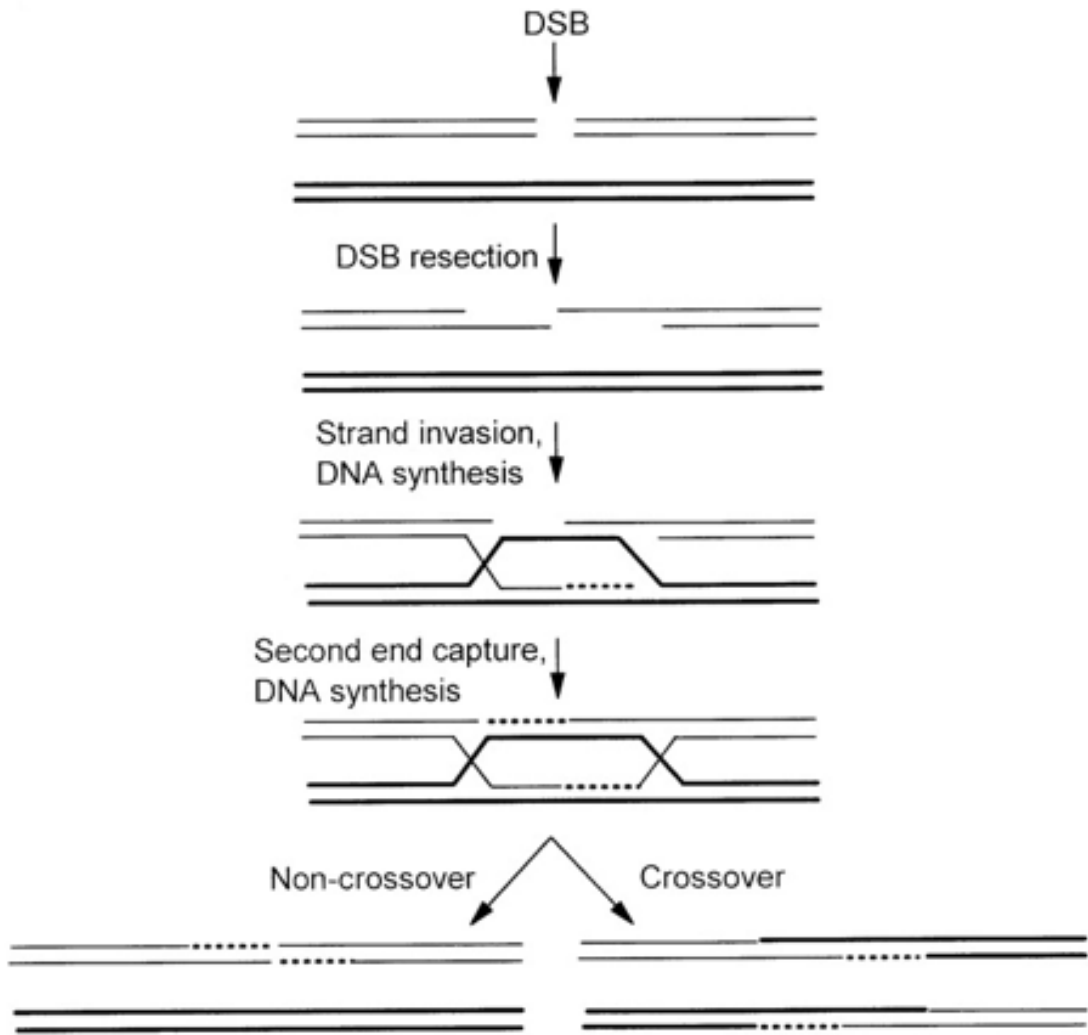


Figure 2. The DSBR model of meiotic recombination. Double strand break initiates homologous recombination. 5' ends are resected to reveal 3' ssDNA overhands. 3' ssDNA invades a homologous region of the homologous chromosome. DNA synthesis, using the homolog as template, forms a joint molecule with a double Holliday junction, which is resolved to form mainly crossover products and sometimes non-crossover products. Figure from Read et al., 2004.

Tian

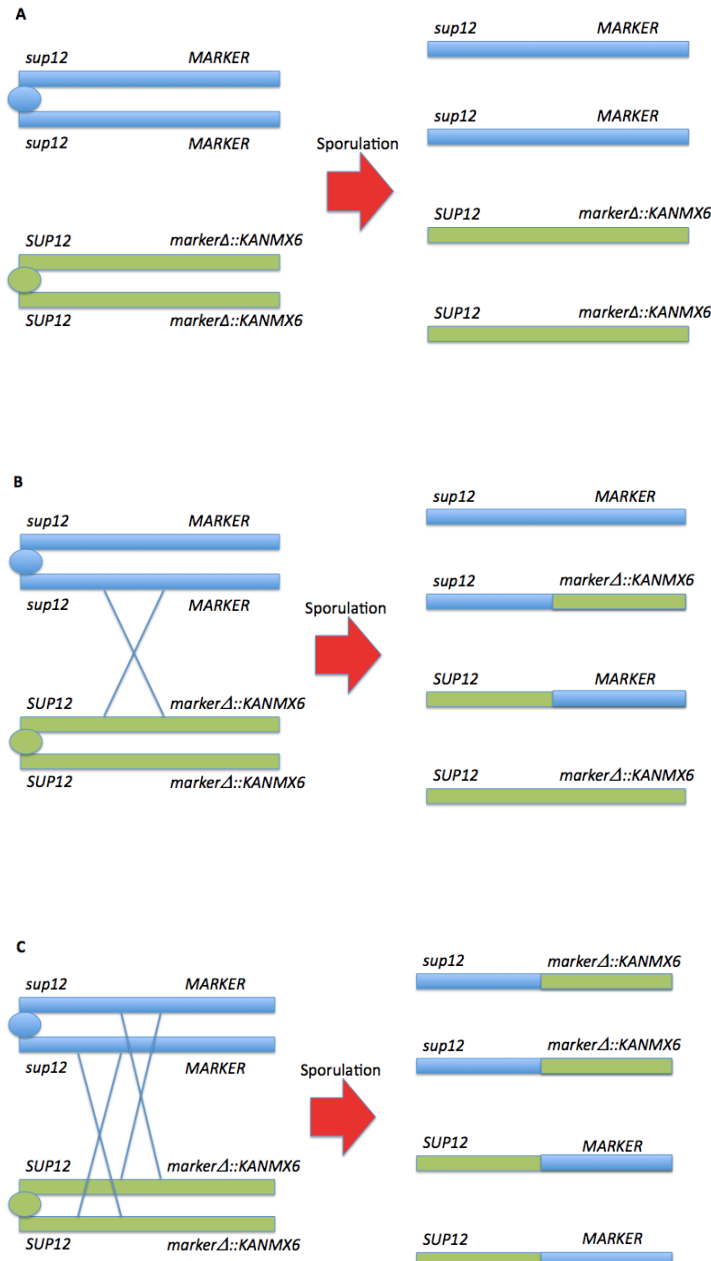


Figure 3. Recombination frequency correlates with the pattern of marker segregation during meiosis. Bars of identical color are sister chromatids after DNA synthesis during meiosis. Different colored bars are homologous chromosomes. Thin crossed lines represent one recombination event. (A) No recombination between *sup12* and the marker gene leads to the parental ditype (PD) segregation pattern. (B) One recombination event leads to two recombinant and two parental type spores, and event termed tetrapatype (T). (C) Two recombination events form four recombinant spores, the non-parental ditype (NPD) pattern. The marker genes conferred resistance to Geneticin. Since both parents were *dmc1Δ*, the presence of *sup12* was scored by mating spores with a *dmc1-ts10 sup12* haploid “tester” strain to check for the suppression phenotype. The Perkins equation was used to convert PD:NPD:T ratios into recombination frequencies.

Tian

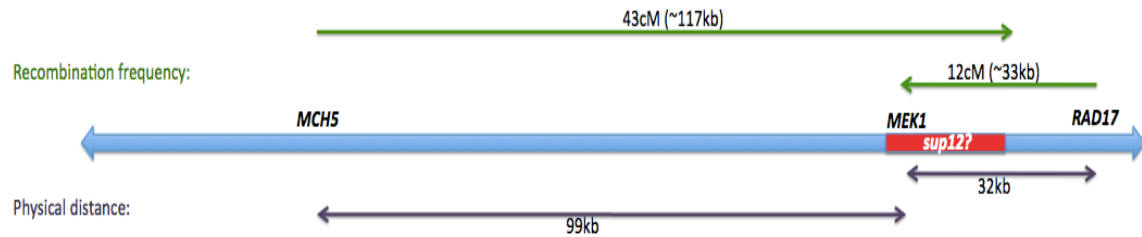


Figure 4. Summary of linkage analysis results indicating putative region containing *sup12*. Recombination frequencies were converted to physical distances between *sup12* and the markers *MCH5*, *MEK1*, and *RAD17* (using the approximate regional conversion factor 2.72kb/cM (see Results), and mapped onto chromosome XV (blue bar). The distance from *MEK1* to *sup12* was not shown because it was calculated to be 0kb. A 20kb region (red bar) that includes the region of overlap of recombination frequencies was the putative location of *sup12* that was subsequently sequenced. All distances are to scale.

Tian

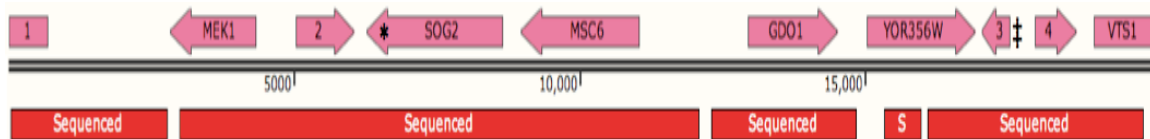


Figure 5. Sequencing 94% of the 20kb region, indicated by linkage analysis to contain *sup12*, revealed two point mutations in the *sup12* strain, but not the wild-type parent of *sup12*. Red bars indicate sequenced regions. Pink bars are ORFs, with 1=*MNE1*, 2=*YOR352W*, 3=*SNX3*, 4=*HAP5*. * indicates a tryptophan 727 to stop codon mutation in *SOG2*. *SOG2* is an integral member of the RAM network, which controls cytokinesis and cell separation. ‡ indicates a guanine to cytosine mutation 92 base pairs upstream of *SNX3*.

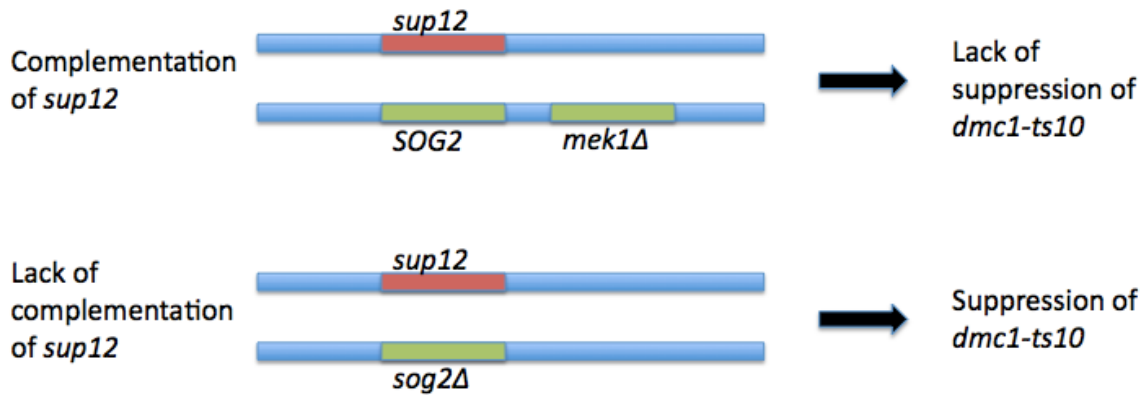


Figure 6. Schematic of the experiment testing whether *sog2Δ* complements *sup12*. Blue bars represent homologous chromosomes. This figure assumes that *sup12* is indeed an allele of *SOG2*. In a *dmc1-ts10* background, because *sup12* is recessive, *sup12/SOG2* (indicated by the *mek1Δ* strain) does not express the *sup12* suppression phenotype (*sup12* is complemented). However, if a *sup12* haploid is mated to a *sog2Δ* haploid, then in the diploid *dmc1-ts10* would be suppressed, since wild-type Sup12 protein (i.e. Sog2p) would not be present in the diploid (*sup12* is not complemented).

Tian

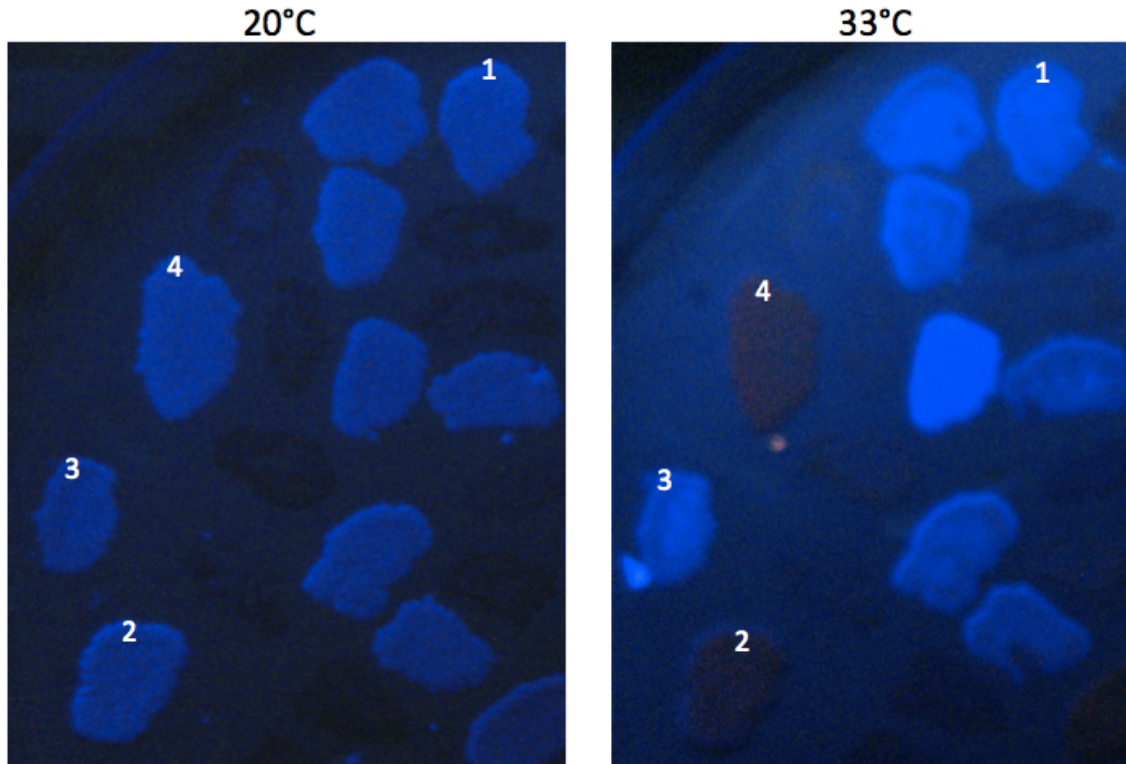


Figure 7. Results of the dityrosine fluorescence assay for *SOG2* strains in the complementation test. Spores, but not vegetative cells, contain dityrosine in their cell walls, which fluoresces blue under ultraviolet light. These colonies were sporulated on SPM + 1/5 COM plates. 1: *sog2Δ/sup12*; 2: *sup12/SUP12*; 3: *sup12/sup12*; 4: *sog2Δ/SUP12* (see Table 4 for details on strains).

Tian

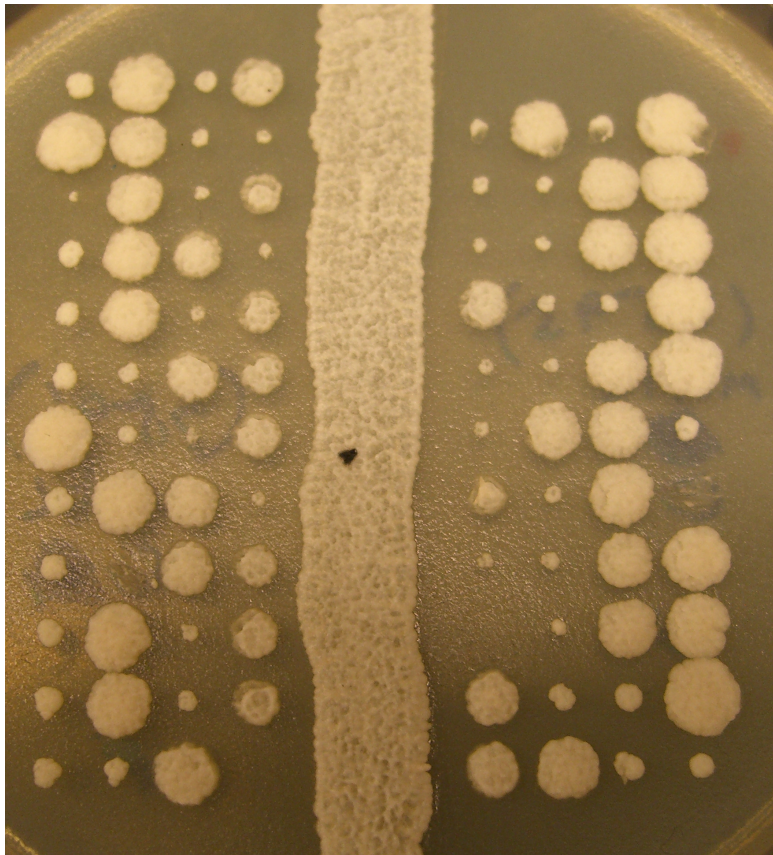


Figure 8. Morphology of *sog2Δ* colonies. *dmc1-ts10 sog2Δ* mutants form smaller colonies than wild-type cells. In this plate of dissected tetrads, all small colonies are *sog2Δ* and all large cells are *SOG2*. The sporulated diploid strain (DKB3589) was heterozygous for *sog2Δ*. Since we see that all *sog2Δ* colonies are similarly small, the large *sog2Δ* colonies seen in subsequent strains, all derived from DKB3589, likely resulted from secondary suppressor mutations (see Discussion).

Tian

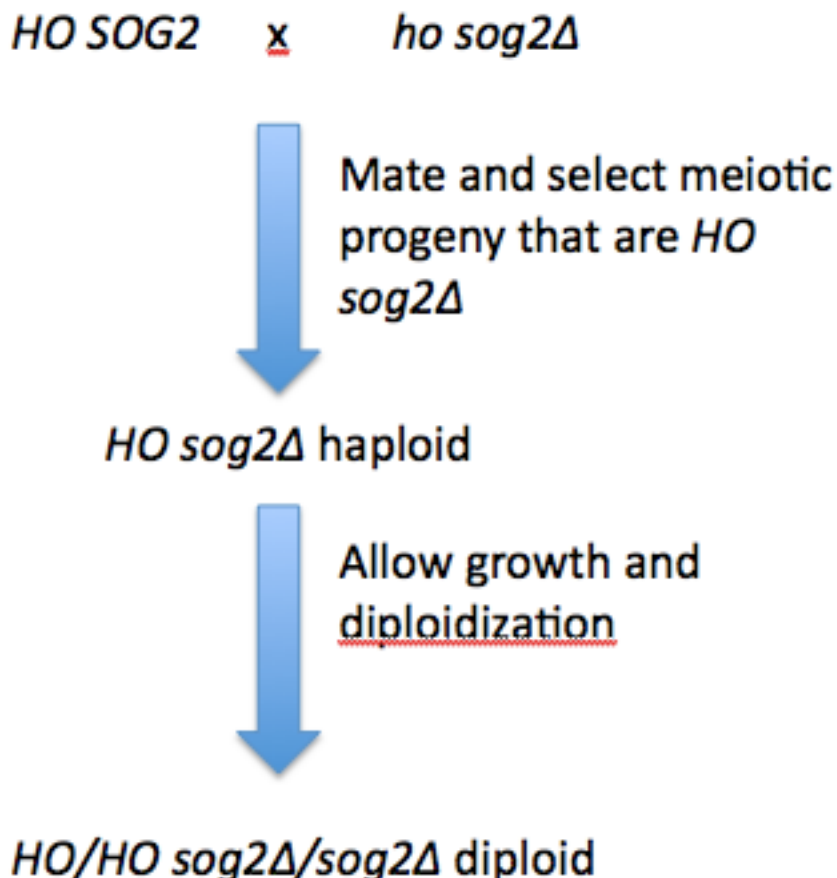


Figure 9. Schematic of the experiment to construct both phenotypically large and small *sog2Δ* diploids in a *HO* background. A *HO SOG2* haploid was mated to a large *ho sog2Δ* haploid. The resulting diploid was sporulated and tetrads were dissected and grown. *HO sog2Δ* spores were isolated by selecting for a prototrophic marker linked to *HO* and an anti-fungicidal marker linked to *sog2Δ*. During growth the *HO sog2Δ* spore diploidized because of the homothallism phenotype. We isolated both large and small *sog2Δ* clones from the cross, indicating that the variance in size phenotypes was caused by one or more extragenic suppressor mutations of *sog2Δ* that were able to segregate independently of *sog2Δ*, rather than by problems with the *SOG2* locus.

Tian

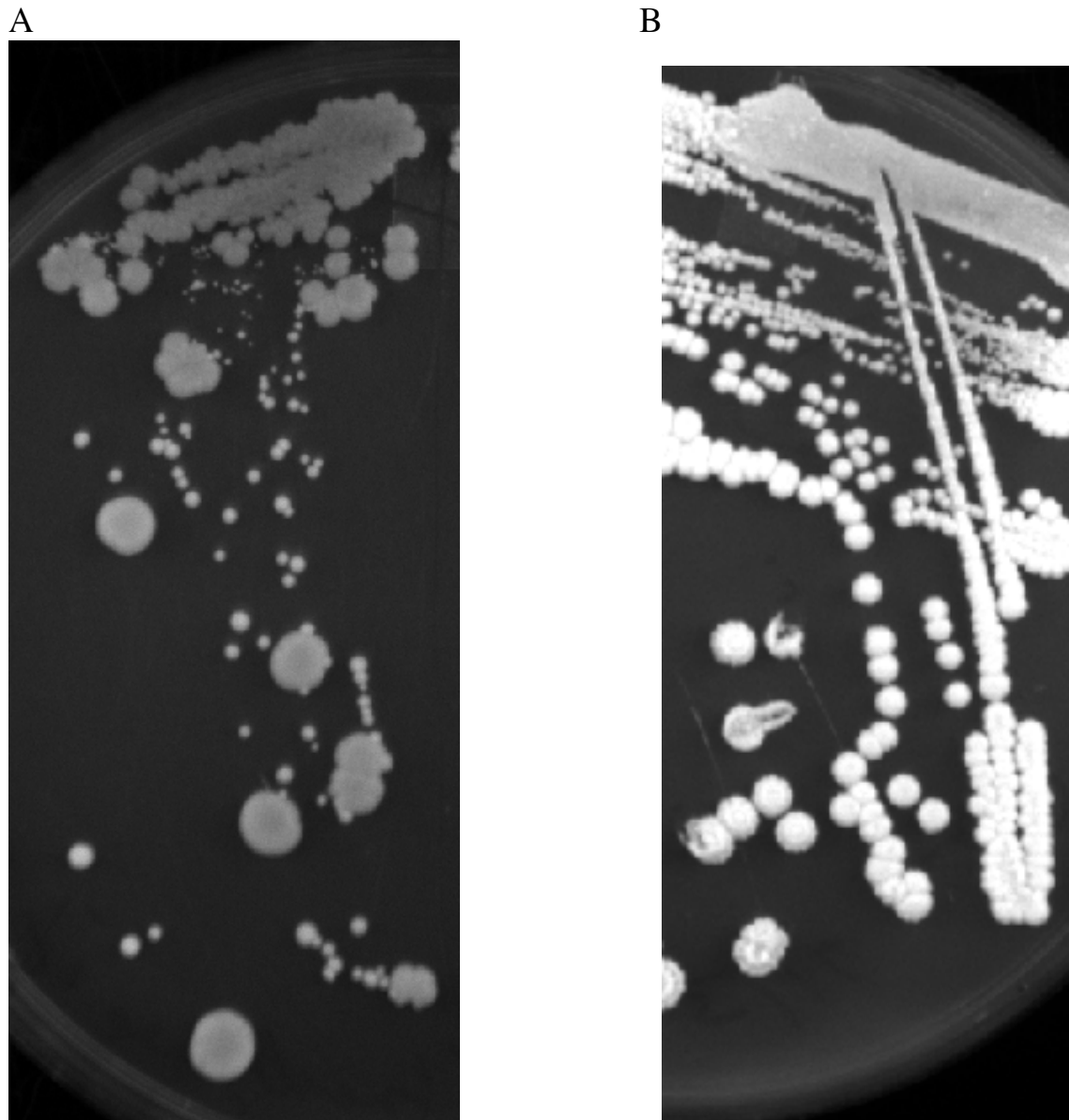


Figure 10. *sog2Δ* mutants displayed varied colony size phenotypes, possibly due to secondary suppressor mutations, while *sup12* mutants did not show varied colony sizes. (A) DKB3679 (large *sog2Δ* single mutant) was crossed to DKB3459 (wild-type), and a spore that was *sog2Δ* and had a small colony phenotype was isolated, grown on YPDA and saved to -80°C. The clone was later resuscitated by streaking onto YPDA. The streaked plate is pictured above and the abundance of large colonies indicates that suppression mutations accumulated between the original isolation of the small spore and

Tian

the streaking shown here. Growth was for 3 days at 30°C and 2 days at room temperature. (B) Shown for comparison is DKB2704 (*dmc1-ts10 sup12*) streaked onto YPDA from -80°C and grown for 3 days at 30°C, then stored at 4°C. *sup12* mutants did not exhibit the variety of colony sizes that *sog2Δ* mutants did. Sizes between the two pictures should not be compared, as growth durations were different.

TABLES

Table 1. Yeast strains

Linkage analysis

DKB #	MA T	Genotype
3381	a	<i>ho::LYS2, lys2, ura3, leu2::hisG, his4X, arg4, ADE2-dmc1-ts10, dmc1Δ::ARG4, pex11Δ::KANMX6</i>
3382	a	<i>ho::LYS2, lys2, ura3, leu2::hisG, his4X, arg4, ADE2-dmc1-ts10, dmc1Δ::ARG4, arg1Δ::KANMX6</i>
3383	a	<i>ho::LYS2, lys2, ura3, leu2::hisG, his4X, arg4, ADE2-dmc1-ts10, dmc1Δ::ARG4, sti1Δ::KANMX6</i>
3384	a	<i>ho::LYS2, lys2, ura3, leu2::hisG, his4X, arg4, ADE2-dmc1-ts10, dmc1Δ::ARG4, leu9Δ::KANMX6</i>
3385	a	<i>ho::LYS2, lys2, ura3, leu2::hisG, his4X, arg4, ADE2-dmc1-ts10, dmc1Δ::ARG4, his3Δ::KANMX6</i>
3386	a	<i>ho::LYS2, lys2, ura3, leu2::hisG, his4X, arg4, ADE2-dmc1-ts10, dmc1Δ::ARG4, rad17Δ::KANMX6</i>
3445	a	<i>ho::LYS2, lys2, ura3, leu2::hisG, his4X, arg4, ADE2-dmc1-ts10, dmc1Δ::ARG4, mch5Δ::KANMX6</i>
3528	a	<i>ho::hisG or ho::LYS2, LYS2 or lys2 (phenotype Lys+), ura3, leu2::hisG, arg4, ADE2-dmc1-ts10, dmc1Δ::ARG4, his4-X, mek1Δ::NAT</i>

Other strains

DKB #	MA T	Genotype
17	a/α	<i>HO/”, ade2::TnLK/”, leu2::hisG/”, lys2/”, ura3Δ::hisG/”, ste7-1/”</i>
793	a	<i>ho::LYS2, lys2, ura3, arg4, his4X, leu2::hisG, dmc1Δ::ARG4</i>
794	α	<i>ho::LYS2, lys2, ura3, arg4, his4X, leu2::hisG, dmc1Δ::ARG4</i>

Tian

1931	a	<i>ho::LYS2, lys2, ura3, leu2::hisG, his4X, arg4, ADE2-dmc1-ts10, dmc1Δ::ARG4</i>
1946	a/α	<i>ho::LYS2/”, lys2/”, ura3/”, leu2::hisG/”, his4X/”, arg4/”, ADE2-dmc1-ts10/”, dmc1Δ::ARG4/”</i>
2193	a	<i>ho::LYS2, lys2, arg4, leu2::hisG, his4X, dmc1Δ::ARG4, ADE2-dmc1-ts10</i>
2197	a/α	<i>ho::LYS2/”, lys2/”, arg4/”, leu2::hisG/”, his4X/his4B, dmc1Δ::ARG4/”, ADE2-dmc1-ts10/”</i>
2604	a/α	<i>HO/”, lys2/”, his4X/”, leu2::hisG/”, ura3/”, arg4/”, ADE2-dmc1-ts10/”, dmc1Δ::ARG4/”, ste7-1/”</i>
2677	a/α	<i>HO/”, lys2/”, his4X/”, leu2::hisG/”, ura3/”, arg4/”, ADE2-dmc1-ts10/”, dmc1Δ::LEU2/”, ste7-1/”, sup12/”</i>
2702	α	<i>ho::LYS2, lys2, ura3, leu2::hisG, his4X, arg4, ADE2-dmc1-ts10, dmc1Δ::ARG4, sup12</i>
2704	a/α	<i>ho::LYS2/”, lys2/”, ura3/”, leu2::hisG/”, his4X/his4B, arg4/”, ADE2-dmc1-ts10/”, dmc1Δ::ARG4/”, sup12/”</i>
3012	α	<i>ho::LYS2, lys2, ura3, leu2::hisG, his4X, arg4, ADE2-dmc1-ts10, dmc1Δ::ARG4, trp5::URA3, sup12</i>
3013	a	<i>ho::LYS2, lys2, ura3, leu2::hisG, his4B, arg4, ADE2-dmc1-ts10, dmc1Δ::ARG4, trp5::URA3, sup12</i>
3326	α	<i>leu2::hisG, his4-X::LEU2-(NgoMIV + ori)-ura3, ho::hisG, ura3, mek1Δ::NAT</i>
3459	a	<i>ho::hisG, leu2::hisG, ura3, HIS4::LEU2-(BamHI; +ori)</i>
3518	a/α	<i>HO/”, lys2/”, his4X/”, leu2::hisG/”, ura3/”, arg4/”, ADE2-dmc1-ts10/”, dmc1Δ::LEU2/”, ste7-1/”, sup12/”</i>
3529	α	<i>ho::LYS2, ura3, LEU2 or leu2::hisG, arg4, ADE2-dmc1-ts10, dmc1Δ::ARG4, his4X or his4X::LEU2 (Leu+ phenotype), mek1Δ ::NAT</i>
3587	α	<i>ho::hisG, leu2::hisG, ura3, HIS4::LEU2-(BamHI; +ori), arg4, lys2, ade2</i>
3588	α	<i>ho::hisG, leu2::hisG, ura3, his4-X::LEU2-(NgoMIV; +ori)-URA3, arg4, lys2, ade2</i>
3589	a/α	<i>ho::LYS2/”, lys2/”, arg4/”, leu2::hisG/”, his4X/his4B, dmc1Δ::ARG4/”, ADE2-dmc1-ts10/”, sog2Δ::KANMX4/SOG2</i>

Tian

3592	a/α	<i>ho::LYS2/”, lys2/”, arg4/”, leu2::hisG/”, his4X/his4B, dmc1Δ::ARG4/”, ADE2-dmc1-ts10/”, msc6Δ::KANMX6/MSC6</i>
3595	a	<i>ho::LYS2, lys2, arg4, leu2::hisG, his4X or his4B, dmc1Δ::ARG4, ADE2-dmc1-ts10, sog2Δ::KANMX4</i>
3596	α	<i>ho::LYS2, lys2, arg4, leu2::hisG, his4X or his4B, dmc1Δ::ARG4, ADE2-dmc1-ts10, sog2Δ::KANMX4</i>
3597	a	<i>ho::LYS2, lys2, arg4, leu2::hisG, his4X or his4B, dmc1Δ::ARG4, ADE2-dmc1-ts10, msc6Δ::KANMX6</i>
3598	α	<i>ho::LYS2, lys2, arg4, leu2::hisG, his4X or his4B, dmc1Δ::ARG4, ADE2-dmc1-ts10, msc6Δ::KANMX6</i>
3621	a/α	<i>ho::LYS2/”, lys2/”, arg4/”, URA3/ura3, leu2::hisG/”, his4X or his4B/ his4X, dmc1 ::ARG4/”, ADE2-dmc1-ts10/”, sog2Δ::KANMX4/SOG2, SUP12/sup12</i>
3623	a/α	<i>ho::LYS2/”, lys2/”, ura3/”, leu2::hisG/”, his4X/”, arg4/”, ADE2-dmc1-ts10/”, dmc1 ::ARG4/”, TRP5/trp5::URA3, SUP12/sup12</i>
3624	a/α	<i>ho::LYS2/”, lys2/”, arg4/”, leu2::hisG/”, his4X or his4B/”, dmc1 ::ARG4/”, ADE2-dmc1-ts10/”, sog2Δ::KANMX4/”</i>
3625	a/α	<i>ho::LYS2/”, lys2/”, ura3/URA3, leu2::hisG/”, his4X/his4X or his4B, arg4/”, ADE2-dmc1-ts10/”, dmc1 ::ARG4/”, sup12/SUP12, MSC6/ msc6Δ::KANMX6</i>
3626	a/α	<i>ho::LYS2/”, lys2/”, arg4/”, leu2::hisG/”, his4X or his4B/”, dmc1Δ::ARG4/”, ADE2-dmc1-ts10/”, msc6Δ::KANMX6/”</i>
3627	a/α	<i>ho::LYS2/ho:hisG (or LYS2?), lys2/LYS2 (or lys2), ura3/”, leu2::hisG/”, his4X/his4X, arg4/”, ADE2-dmc1-ts10/”, dmc1Δ::ARG4/”, trp5::URA3/ TRP5, sup12/SUP12, MEK1/mek1Δ::NAT</i>
3674	α	<i>ho::LYS2, ura3, HIS4::LEU2-(BamHI; +ori), lys2, leu2::hisG, arg4, ade2, sog2Δ::KANMX4 (large phenotype)</i>
3676	a	<i>ho::LYS2, his4X or his4B, lys2, leu2::hisG, arg4, ade2, sog2Δ::KANMX4 (large phenotype)</i>
3679	α	<i>ho::hisG, leu2::hisG, arg4, lys2, ade2, ura3, his4-X::LEU2-(NgoMIV; +ori)-URA3, sog2Δ::KANMX4 (large phenotype)</i>
3698	a/α	<i>ho::hisG/”, leu2::hisG/”, ura3/’, HIS4::LEU2-(BamHI; +ori)/his4-X::LEU2-(NgoMIV; +ori)-URA3</i>

Table 2. Primers

Table 2-1. Linkage analysis marker construction

oliD B	Primer Name	Primer Sequence (5' - 3')	Primary Use
409	pex11 fw	TGGGTCGTCCCTGGGTTGTT TTCC	PCR up pex11 from KO collection
410	pex11 rev	AGGGTCGAATCAAACATAA GC GGAG	PCR up pex11 from KO collection
411	arg1 fw	CCATTGTGCAGCGATAAGG AACATTG	PCR up arg1 from KO collection
412	arg1 rev	ACGATATTGGGATTTCGC TACGTCA	PCR up arg1 from KO collection

Tian

413	sti1 fw	GCCCAAAAGTCTGCTCCCA AATTCC	PCR up sti1 from KO collection
414	sti1 rev	AGCTTAGCGAACATGTTGTCA TGGAGC	PCR up sti1 from KO collection
415	leu9 fw	ACGAAATCACAAATCCTTGT TTTCGGC	PCR up leu9 from KO collection
416	leu9 rev	CGAAAGAAACTTCCACA CAGACATCG	PCR up leu9 from KO collection
417	his3 fw	CGCTGCACGGTCCTGTTCC C	PCR up his3 from KO collection
418	his3 rev	CGCCACGGCCACCGTTGTA G	PCR up his3 from KO collection
419	mch5 fw	ACTAAGATCACGGGGCAT ACTATCG	PCR up mch5 from KO collection
420	mch5 rev	GAACGAACTCGCAAAATG GCTTCGT	PCR up mch5 from KO collection
421	rad17 fw	AGAAGCCAAGACCCCCGG TT	PCR up rad17 from KO collection
422	rad17 rev	AATGTCTGACGTTGAAGAA GTCGTTGA	PCR up rad17 from KO collection
423	pex11 fw2	CCAAGGCTTCGTCACCACC CA	To check transformation of pex11 into SK1. It is located outside of the transformed construct.
424	arg1 fw2	CCACATGGGCCAGCCACT G	To check transformation of arg1 into SK1. It is located outside of the transformed construct.
425	sti1 fw2	TGCTGGAACCTACAAACCC GCA	To check transformation of sti1 into SK1. It is located outside of the transformed construct.
426	leu9 fw2	CGCGCCATCATGGTCCGGT A	To check transformation of leu9 into SK1. It is located outside of the transformed construct.
427	his3 fw2	CGACGTGGGCCTTTCTT GCC	To check transformation of his3 into SK1. It is located outside of the transformed construct.

Tian

428	mch5 fw2	AACCTGCTGCGCGCTGTTC T	To check transformation of mch5 into SK1. It is located outside of the transformed construct.
429	rad17 fw2	GGATCCTGCCATTGTTTCC AACCG	To check transformation of rad17 into SK1. It is located outside of the transformed construct.

Table 2-2. Sequencing of 20kb region likely containing sup12

oliD B	Primer Name	Primer Sequence (5' - 3')	Primary Use
430	1fw	TGCAGTGAGCGCTGGAGC AA	Amplify and sequence putative region containing sup12
431	1A	CCGCAGCAAAATTATATTTC CGCATC	Sequence putative region containing sup12
432	1B	AATGAATCTTGCTTGAGAG GTTCGAAA	Sequence putative region containing sup12
433	1C	GCAGGATTATCGGATGTAC GAAGCT	Sequence putative region containing sup12
434	1rev	TGCGACGTTATTGAATTAT CGCAGGG	Amplify and sequence putative region containing sup12
435	2fw	TGGTCTACTTCCCTCAGAA AACCCATT	Amplify and sequence putative region containing sup12
436	2A	TGCACAGGACCCCTCTTG CAT	Sequence putative region containing sup12
437	2B	ACGGCTATGCCAGTCTTAC TCC	Sequence putative region containing sup12
438	2C	GCGCTTACTGATACAGCCT TGTATGAA	Sequence putative region containing sup12
439	2rev	TCACTTGCCCCAAGCGCA AATAC	Amplify and sequence putative region containing sup12
440	3fw	ACCATCGAAAGATGTTGC AGAGGTTT	Amplify and sequence putative region containing sup12
441	3A	GTTCAGGTGAAAAGTAGC ATGGAGTT	Sequence putative region containing sup12

Tian

442	3B	CTTTCAACCTTCATAA TCGGTGGG	Sequence putative region containing sup12
443	3C	AATCACGTCTCTTCTTCA AGAGAGC	Sequence putative region containing sup12
444	3rev	ACTTCATGCGCATTAGTAT AGAGCGT	Amplify and sequence putative region containing sup12
445	4fw	CGCAAGGGATTATGGAAG AAGAACCT	Amplify and sequence putative region containing sup12
446	4A	CAGCAAGCGGGATTATATA AAGAAACG	Sequence putative region containing sup12
447	4B	GGTCTAATTCATCTCCTAG AAGGATGC	Sequence putative region containing sup12
448	4C	CACCAGTTAATAGTGCAG CTGCTTC	Sequence putative region containing sup12
449	4rev	GCCCACAGTGACCAGCCC AT	Amplify and sequence putative region containing sup12
450	5fw	AGCTCATACCATGGGGTAC CCGT	Amplify and sequence putative region containing sup12
451	5A	AGGTTCTGCCAGCAGGT GT	Sequence putative region containing sup12
452	5B	TCAGCTGTTCTGCCGTCC TCT	Sequence putative region containing sup12
453	5C	TGGGCCACTACAAGGAGA TAATGATCC	Sequence putative region containing sup12
454	5rev	AGGCTCAGCCGACTTGG CCT	Amplify and sequence putative region containing sup12
455	fw8649 _20kb	ACGGATACTTATAGACTTA ACTCCCC	Sequence putative region containing sup12
456	rev935 7_20kb	CGCAGAGTTAATAAGCCT GACGGCA	Sequence putative region containing sup12
457	rev892 3_20kb	CCAATTCTGCACATATG ATGCTG	Sequence putative region containing sup12
458	fw9203 _20kb	TCGATGTAGGGAACGTAC TCGC	Sequence putative region containing sup12

Tian

459	rev963 7_20kb	ATCAGATGGTGTGTTACCC CCTACT	Sequence putative region containing sup12
460	fw7227 _20kb	TACTACTGGACGATGTCTC GTGCC	Sequence putative region containing sup12
461	fw_152 94_20k b	TCAGGAACAGGCCAATTG CGT	Sequence putative region containing sup12
462	fw_118 88_20k b	AGGGATTATGGAAGAAGA ATCCTTT	Sequence putative region containing sup12
463	fw_146 93_20k b	AACCGTTAGAGGTGGACT AATT	Sequence putative region containing sup12
464	rev_64 08_20k b	ATCGTAATGAGCGACGTG CCTA	Sequence putative region containing sup12
465	rev_12 842_20 kb	GATTATGAAAAGTTGAAA TATCCTGGA	Sequence putative region containing sup12
466	fw_618 2_20kb	AAGCATAACATTTCAGTACC ATGGG	Sequence putative region containing sup12

Table 2-3. *sog2Δ* strain construction

oliD B	Prim er Name	Primer Sequence (5' - 3')	Primary Use
467	KAN MX4 fw KO	CGTAACGTATGGGTAAG GAAAAGACT	Has partial homology to both KANMX4 and sequence upstream of SOG2. Used to amplify KANMX4 and to link it to the sequence amplified from upstream of SOG2
468	KAN MX4 rev KO	CATTACGTATTCTAAAGT TCGCCTTTCTCACAAATG CAAGTTGTCAGTACTGAT TAGA	Has partial homology to KANMX4 and a 40bp sequence downstream of SOG2. Used to amplify KANMX4. Also the 40bp homology arm allows for targeted transformation of the fusion cassette replacing SOG2.

Tian

469	SOG2 fw KO	GGCCACATTGCACGCA ATAC	Used to amplify a 0.5kb sequence upstream of SOG2
470	SOG2 rev KO	CCTTACCCATACGTTACG GATACTTATA	Has partial homology to both KANMX4 and 0.5kb sequence upstream of SOG2. Used to amplify the sequence and to link it to KANMX4.
471	SOG2 fw2 KO	TGGTGTGTTACCCCCCTAC TTTGGAA	Used to test proper transformation of the KANMX4 cassette. It is located outside of the transformed construct.

Table 2-4. *msc6Δ* strain construction

Primer ID	Primer Name	Primer Sequence (5' - 3')	Primary Use
472	MSC 6 fw	GCCGCCGATGCAGAAA ACCG	Amplify msc6 from KO collection
473	MSC 6 rev	TGTGCAGAAAATTGGTT CTGAGCTTT	Amplify msc6 from KO collection
474	msc6 rev2	TTCCTCCTTCGGATCCA ACGTCC	Used to test proper transformation. Located downstream of transformed construct.

Table 3. Recombination frequencies between *sup12* and eight markers that span chromosome XV.

Marker strain (DKB#)	Marker gene	Position of marker on Ch. XV (kb from start)	PD	NP D	T	Recombination frequency ± standard error (cM)
3381	<i>pex11Δ::KANMX</i> 6	53	3	2	11	72 ± 22
3382	<i>arg1Δ::KANMX6</i>	219	2	2	7	86 ± 31
3383	<i>sti1Δ::KANMX6</i>	383	2	3	11	91 ± 26
3384	<i>leu9Δ::KANMX6</i>	526	2	3	5	115 ± 39
3385	<i>his3Δ::KANMX6</i>	722	2	1	10	62 ± 20
3445	<i>mch5Δ::KANMX6</i>	901	10	1	24	43 ± 8
3528	<i>mek1Δ::NAT</i>	1000	28	0	0	0 ± 0
3386	<i>rad17Δ::KANMX</i> 6	1032	77	0	23	12 ± 2

Tian

The linkage analysis strategy used to determine the recombination frequencies is described in Fig. 3. Recombination frequencies were calculated using the Perkins equation. The parental ditype:non-parental ditype:tetratype (PD:NPD:T) ratio between two unlinked genes is 1:1:4, which gives a recombination frequency of 83% by the Perkin's equation. Marker positions along Ch. XV were found at the SGR Project (http://www.sanger.ac.uk/cgi-bin/blast/submitblast/s_cerevisiae_sgpr).

Table 4. Complementation test between knockouts of candidates for *SUP12* identity (*SOG2*, *MSC6*, and *MEK1*) and *sup12*.

			Sporulation observed?	
	Strain (DKB#)	Genotype	20°C	33°C
<i>SOG2</i> strains	3621	<i>sog2Δ/SOG2</i> <i>SUP12/sup12</i>	Yes	Yes
	3589	<i>sog2Δ/SOG2</i> <i>SUP12/SUP12</i>	Yes	No
	3624	<i>sog2Δ/sog2Δ</i> <i>SUP12/SUP12</i>	Yes	Inconclusiv e ^a
<i>MSC6</i> strains	3625	<i>msc6Δ/MSC6</i> <i>SUP12/sup12</i>	Yes	No
	3592	<i>msc6Δ/MSC6</i> <i>SUP12/SUP12</i>	Yes	No

Tian				
	3626	<i>msc6Δ/msc6Δ</i> <i>SUP12/SUP12</i>	Yes	No
MEK1 strains	3627	<i>mek1Δ/MEK1</i> <i>SUP12/sup12</i>	Yes	No
	3529 x 2193	<i>mek1Δ/MEK1</i> <i>SUP12/SUP12</i>	Yes	No
	3628 & 3629	<i>mek1Δ/mek1Δ</i> <i>SUP12/SUP12</i>	Yes	Yes ^b
sup12 controls	3623	<i>sup12/SUP12</i>	Yes	No
	2704	<i>sup12/sup12</i>	Yes	Yes

For the logic behind this experiment see Fig. 6. All strains were in a *dmc1-ts10* background. Lack of complementation was detected by suppression of *dmc1-ts10*. Sporulation was assayed using the dityrosine fluorescence assay (for example plate see Fig. 7). The *sog2Δ/sup12* strain sporulated at 33°C, indicating that *sup12* is an allele of *SOG2*. *msc6Δ/sup12* and *mek1Δ/sup12* strains did not sporulate at 33°C, indicating that those two genes close to *SOG2* are not *SUP12*. Importantly all strains sporulated at the permissive temperature (20°C), indicating that any lack of sporulation at the restrictive temperature was because of complementation, and not a meiotic defect from strain construction. ^aWe do not have conclusive results yet. A first trial showed sporulation, but a second trial did not (see Results for details). ^bThis result was expected, since *mek1* mutants have been shown to bypass the need for Dmc1 (Xu et al., 1997).

Table 5. Spore viability of *sog2Δ* and *sup12* mutants in a homozygous *dmc1-ts10* background.

Strain (DKB#)	Genotype	Proportion of spores that germinated at:	
		20°C	33°C
1946	<i>SOG2/SOG2</i> <i>SUP12/SUP12</i>	63/64 (98%)	Insufficient sporulation
3589	<i>sog2Δ/SOG2</i> <i>SUP12/SUP12</i>	70/72 (97%)	Insufficient sporulation

Tian

3012 x 1931	<i>SOG2/SOG2</i> <i>sup12/SUP12</i>	73/76 (96%)	Insufficient sporulation
2704	<i>SOG2/SOG2</i> <i>sup12/sup12</i>	42/48 (88%) ^a	70/92 (76%) ^b
3595 x 2702	<i>sog2Δ/SOG2</i> <i>SUP12/sup12</i>	9/68 (13%) ^c	12/48 (25%) ^d
3595 x 3596	<i>sog2Δ/sog2Δ</i> <i>SUP12/SUP12</i>	6/84 (7%) ^e	14/92 (15%) ^{f,g}

Meiosis was induced in the diploids and tetrads were dissected and grown on nutrient-rich medium (YPDA). Spore viability is the proportion of spores that germinated after tetrad dissection and grew into a colony. Spore viability patterns: ^a2-spore: 1; 3-spore: 4. ^b1-spore: 2; 2-spore: 5; 3-spore: 6. ^c1-spore: 5; 2-spore: 2. ^d1-spore: 1; 2-spore: 3; 3-spore: 1. ^e1-spore: 6. ^f1-spore: 7; 2-spore: 2; 3-spore: 1. ^gIt is unclear whether *sog2Δ* diploids are actually able to suppress *dmc1-ts10*, since results were inconsistent when the experiment was repeated (see Table 4 and Results); the tetrads used here were from the first trial when sporulation was successful at 33°C.

Table 6. Spore viability of homozygous *sog2Δ* single mutants

Homothallic?	Strain (DKB#)	Genotype	Proportion of spores that germinated:	
			First trial	Second trial
Yes	All are spores from 3676 x 17	<i>sog2Δ/sog2Δ</i> (large)	71/76 (93%)	Did not analyze
		<i>sog2Δ/sog2Δ</i> (small)	40/92 (43%) ^a	13/118 (11%) ^b

Tian

	SOG2/SOG2	89/93 (96%)	82/88 (93%)
3674 x 3676 and 3679 x 3676	<i>sog2Δ/sog2Δ</i> (large)	110/116 (95%)	
No	None	<i>sog2Δ/sog2Δ</i> (small)	Strain was not constructed
3679 x 3459	<i>sog2Δ/SOG2</i>	102/108 (94%)	
3698	<i>SOG2/SOG2</i>	86/88 (98%)	

Meiosis was induced in the diploids and tetrads were dissected and grown on nutrient-rich medium (YPDA). Spore viability is the proportion of spores that germinated and grew into a colony. Strains in the *HO/HO* (homothallic) background were constructed using the strategy outlined in Fig. 9 that took advantage of the homothallism phenotype. Strains in the *ho/ho* background were constructed by mating two haploids that had the desired *SOG2* allele. The second trial using the *HO/HO* strains occurred after freezing the strains at -80°C and resuscitation on nutrient rich medium (YPDA). The *ho sog2Δ* diploid was not constructed because small *sog2Δ* segregants were difficult to obtain and maintain (see Discussion). ^aCombined results from two clones. Viability pattern: 0-spore: 6; 1-spore: 4; 2-spore: 3; 3-spore: 6; 4-spore: 4. ^bCombined results from two clones. Viability pattern: all growth was in the form of one-spore tetrads.